Science of the Total Environment 548–549 (2016) 289–306

Contents lists available at ScienceDirect

Science of the Total Environment

journal homepage: www.elsevier.com/locate/scitotenv

An appraisal of precipitation distribution in the high-altitude catchments of the Indus basin

Zakir Hussain Dahri [a,b,*], Fulco Ludwig [b], Eddy Moors [c,d], Bashir Ahmad [a], Asif Khan [e,f,g], Pavel Kabat [b,g]

[a] Climate Change Alternate Energy and Water Resources Institute, National Agricultural Research Centre (NARC), Pakistan Agricultural Research Council, Islamabad, Pakistan
[b] Earth System Science, Wageningen University, P.O. Box 47, 6700 AA Wageningen, The Netherlands
[c] Climate Change and Adaptive Land & Water Management, Alterra Wageningen UR, P.O. Box 47, 6700 AA Wageningen, The Netherlands
[d] Earth and Climate Cluster, Faculty of Earth and Life Sciences. VU University Amsterdam, The Netherlands
[e] Department of Engineering, University of Cambridge, Trumpington Street, Cambridge CB2 1PZ, United Kingdom
[f] Department of Engineering, University of Engineering and Technology, Peshawar, Pakistan
[g] International Institute for Applied Systems Analysis, Schlossplatz 1, A-2361 Laxenburg, Austria

HIGHLIGHTS

- We developed an improved estimation of precipitation distribution over the upper Indus basin.
- Results show clear non-linear increases in precipitation with altitude.
- The estimated precipitation is much higher compared to previous studies and gridded products.
- The gridded precipitation products are unsuitable to force hydrological models in upper Indus.
- The basin-wide seasonal and annual correction factors can be used for hydrological models.

GRAPHICAL ABSTRACT

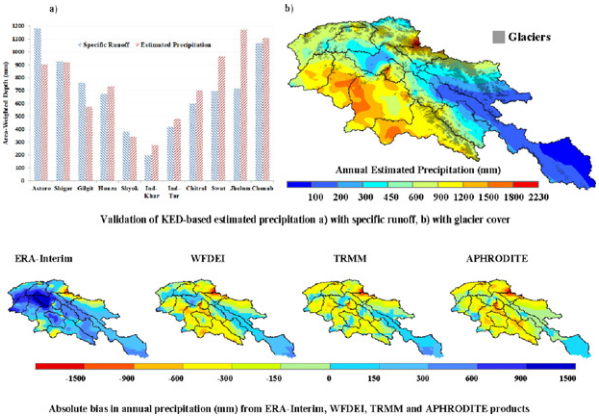

ARTICLE INFO

Article history:
Received 26 June 2015
Received in revised form 31 December 2015
Accepted 1 January 2016
Available online 21 January 2016

Editor: D. Barcelo

Keywords:
Indus basin
Precipitation distribution
High-altitude areas
Gridded precipitation products
Bias correction

ABSTRACT

Scarcity of in-situ observations coupled with high orographic influences has prevented a comprehensive assessment of precipitation distribution in the high-altitude catchments of Indus basin. Available data are generally fragmented and scattered with different organizations and mostly cover the valleys. Here, we combine most of the available station data with the indirect precipitation estimates at the accumulation zones of major glaciers to analyse altitudinal dependency of precipitation in the high-altitude Indus basin. The available observations signified the importance of orography in each sub-hydrological basin but could not infer an accurate distribution of precipitation with altitude. We used Kriging with External Drift (KED) interpolation scheme with elevation as a predictor to appraise spatiotemporal distribution of mean monthly, seasonal and annual precipitation for the period of 1998–2012. The KED-based annual precipitation estimates are verified by the corresponding basin-wide observed specific runoffs, which show good agreement. In contrast to earlier studies, our estimates reveal substantially higher precipitation in most of the sub-basins indicating two distinct rainfall maxima; 1st along southern and lower most slopes of Chenab, Jhelum, Indus main and Swat basins, and 2nd around north-west corner of Shyok basin in the central Karakoram. The study demonstrated that the selected gridded precipitation products covering this region are prone to significant errors. In terms of quantitative estimates, ERA-Interim is relatively

* Corresponding author at: Earth System Science, Wageningen University, P.O. Box 47, 6700 AA Wageningen, The Netherlands and Climate Change Alternate Energy and Water Resources Institute, National Agricultural Research Centre (NARC), Pakistan Agricultural Research Council, Islamabad, Pakistan.
E-mail addresses: zakir.dahri@wur.nl, zakirdahri@yahoo.com (Z.H. Dahri).

http://dx.doi.org/10.1016/j.scitotenv.2016.01.001

close to the observations followed by WFDEI and TRMM, while APHRODITE gives highly underestimated precipitation estimates in the study area. Basin-wide seasonal and annual correction factors introduced for each gridded dataset can be useful for lumped hydrological modelling studies, while the estimated precipitation distribution can serve as a basis for bias correction of any gridded precipitation products for the study area.

1. Introduction

The Hindukush Karakoram Himalayan (HKH) mountain region and adjoining ranges of Pamirs and Tibetan Plateau (TP) hold the world's largest repositories of snow and ice mass outside the Polar Regions (Qiu, 2008; UNESCO-SCOPE-UNEP, 2011). The Indus River System (IRS), originating from TP and HKH mountain region and crossing through China, India, Afghanistan and Pakistan, sustains livelihoods of over 215 million people. Yet, little is known about environmental change and mountain hydrology in this highly diversified and complex mountain region (Immerzeel et al., 2012; Karki et al., 2011). There is limited understanding of quantitative and spatiotemporal distribution of precipitation, which provides the basic and critical input for hydrological assessment, mass balance and climate change studies. The current knowledge is mainly constrained by limited in-situ hydrometeorological and cryospheric mass balance observations in the high-altitude catchments of Indus basin (Pellicciotti et al., 2012; Wake, 1987). Political environments, poor accessibility and harsh weather conditions pose serious challenges for such observations in this region. As a result, there are significant data, information and knowledge gaps in hydro-climatic aspects.

Precipitation in the high-altitude catchments of Indus basin is predominantly controlled by large-scale orography and remains highly variable in time, space and altitude. Its variability and distribution pattern mainly depends on the interactions and interplay of orographic features with large-scale atmospheric circulation systems, regional climatic processes and local evapotranspiration rates. Large changes in precipitation over short distances and within short periods of time are common and high amplitude events are often localized (Nesbitt and Anders, 2009). The zone of maximum precipitation is usually the function of enhanced moisture condensation and exponential reduction in the quantity of available moisture with increasing barrier height (Alpert, 1986). Hence, rainfall gradients in the complex terrains are often not linearly correlated with altitude (Singh and Kumar, 1997; Loukas and Quick, 1996). Nevertheless, several other studies indicated that precipitation in the HKH region exhibits a considerable vertical gradient (e.g. Pang et al., 2014; Winiger et al., 2005; Hewitt, 2011; Weiers, 1995; Wake, 1989; Dhar and Rakhecha, 1981; BIG, 1979; Decheng, 1978).

Precipitation is an important component of the hydrological cycle that governs the renewable water resources affecting agro-economic development, hydropower generation and environmental integrity. Therefore, accurate assessment of precipitation is essential as small errors in precipitation estimates may translate into major changes in surface runoff estimates and associated water allocations. Accurate assessment of precipitation requires good quality observations with adequate spatiotemporal coverage to assess the sub-basin or local scale variability. However, the existing rain gauge network in this region is not only inadequate but also biased towards valley bottoms (Fowler and Archer, 2006). The solid precipitation (snowfall) at higher altitudes is often difficult to accurately measure and generally susceptible to undercatch by 20–50% (Rasmussen et al., 2012). Furthermore, the Indus is an international river basin and the available observational data are usually fragmented and scattered with different organizations in four countries and are not freely accessible. Therefore, there is an ever-increasing trend of using the easily available global and/or regional scale gridded datasets for hydro-climatic assessment and mass balance studies (e.g. Lutz et al., 2014a; Sakai et al., 2014; Immerzeel et al., 2012, 2010, 2009; Tahir et al., 2011; Bookhagen and Burbank, 2006).

Indeed, the gridded datasets provide better information in terms of spatial coverage and temporal consistency, but with potentially large errors particularly in high-mountains where the resolution of the data is often larger than the spatial variability of precipitation and the adopted interpolation schemes add further uncertainty. Also, satellite observations underestimate precipitation in areas with significant snowfall (Andermann et al., 2011). Moreover, the gridded datasets covering the high-altitude areas of Indus basin use station data of only a few commonly available old observatories predominantly located at the valley floors, which do not reflect the topographical complexity and spatial variability of precipitation in these areas (Reggiani and Rientjes, 2015). Hence, the accuracy of gridded datasets is particularly questionable in this region requiring their correction and validation before use. However, the limitations and internal inconsistencies of the gridded datasets are often underestimated or overlooked in the hydro-climate studies; where underestimated precipitation is often compensated by underestimated evapotranspiration and/or overestimated snow/glacier melt rates (Lutz et al., 2014a; Pellicciotti et al., 2012; Schaefli et al., 2005). Ultimately, the inferences regarding precipitation distribution, snow/glacier cover dynamics and associated melt water contributions are inaccurately adjudicated. Point observations, on the other hand, provide relatively accurate local information, but their wider-scale use in hydro-climate studies is constrained by their restricted accessibility, limited spatiotemporal coverage and uneven distribution in both horizontal and vertical directions. Paucity of precipitation measurements in the high-altitude areas, where the bulk of precipitation falls, provides an incomplete picture of precipitation distribution. Auspiciously, there are few mass balance studies (e.g. Mayer et al., 2014, 2006; Hewitt, 2011; Shroder et al., 2000; Bhutiyani, 1999; Wake, 1989; Mayewski et al., 1984, 1983; Kick, 1980; BIG, 1979; Decheng, 1978; Qazi, 1973) that indirectly estimated net precipitation (as water equivalent) using snow pillows, snow pits, and ice cores from the accumulation zones of few important large glaciers in this region. These sparse but relatively accurate and high-altitude point observations can be combined and linked with the low-mid altitude observations to derive high-altitude precipitation and to verify and correct the gridded datasets developed through various means.

In addition, the specific runoffs (measured flow/drainage area) from all the high altitude catchments of Indus basin are significantly higher than the corresponding precipitation estimates by earlier studies (Immerzeel et al., 2012, 2015). This indicates that either the estimated precipitation is lower than the actual or these basins are receiving bulk of their runoff from snow/glacier melt in the absence of an adequate precipitation (snowfall) input to sustain the snow/glacier systems. The latter case certainly recognizes for tangible glacier retreat and loss of glacial mass. However, the scientific research on precipitation inputs and associated snow/glacier mass balance in the study area is uncertain and largely contradicting due mainly to paucity of in-situ precipitation and glacier mass balance data (Kaab et al., 2012; Immerzeel et al., 2009). Moreover, mass balance studies in this region are always difficult as most of the glaciers based at the high-altitude areas (above 4000 m) are often nourished by avalanches and redistribution by wind in addition to seasonal snow (Hewitt, 2013, 2011). While Kaab et al. (2015, 2012), Wiltshire (2014), Gardner et al. (2013), Jacob et al. (2012),

Cogley (2011) and Immerzeel et al. (2009) noticed loss of ice mass and consistent decrease in glacier extent in the HKH region, several other studies (e.g. Bhambri et al., 2013; Minora et al., 2013; Gardelle et al., 2013, 2012; Bolch et al., 2012; Scherler et al., 2011; Tahir et al., 2014, 2011; Schmidt and Nüsser, 2012; Mayer et al., 2006; Hewitt, 2005) indicated 'Karakoram anomaly' advocating stability or even growth of Hindukush–Karakoram glaciers. The possible reasons for such an anomaly have been linked to the role of debris-covered areas in reducing ice ablation (Scherler et al., 2011) and favourable changes in winter precipitation and summer temperatures (Mathison et al., 2013; Hewitt, 2011, 2005; Fowler and Archer, 2006; Archer and Fowler, 2004).

Given the importance of precipitation and a large uncertainty over its distribution, the major aim of this study is to analyse altitude dependency of precipitation and derive its spatiotemporal distribution by using the observed data/information available from different sources. Therefore, we collected precipitation data of 118 meteorological stations; more than half of these are located at mid to high-altitudes and have never been used for formation or calibration of precipitation datasets. These station observations are further supported by 16 virtual stations over major glacier accumulation zones, where average net annual precipitation is estimated through mass balance studies. We focus separately on each sub hydrological basin and explain how precipitation amounts, seasonality and patterns are represented. The study provides much improved estimates of precipitation distribution, which are comparable and consistent with the corresponding observed runoffs from the 12 sub-basins.

2. Study area

The Indus basin originates from the TP and the HKH region and spreads over parts of China (8%), India (39%), Afghanistan (6%) and Pakistan (47%). The study area extends over the high-mountain sub-basins of Indus basin (Fig. 1). The total area of these high-altitude catchments is 259,913 km^2 of which 57.5% is laid above 4000 m a.s.l. Although, there is no definite boundary among the three mountain ranges but it is generally assumed that the river Indus bisects the Himalayan range from the Hindukush, Karakoram and TP. The eastern boundary of Shyok basin limits the Karakoram range in the east, while the boundary between Gilgit and Hunza basins separates it from the Hindukush range. The study area is the largest source of fresh water resources (153 BCM year^{-1}) of Pakistan and plays a crucial role in water, energy and food security of the region.

The extensive Eurasian continent and the Indian and Pacific oceans play an important role in atmospheric circulation and monsoon formation of the world's largest and most powerful monsoon system in South Asia (Saha, 2010). The climate of Indus basin is characteristic of the South Asian atmospheric circulation that is associated with the summer monsoon evolution and extra-tropical cyclonic/anticyclonic circulations around troughs of low/high pressure areas during winter. Thus, precipitation in the study area is predominantly influenced by the two principal weather systems: the Indian summer monsoon (ISM) advecting moisture from the Indian Ocean, Arabian Sea and Bay of Bengal due to the differential heating between land and sea during summer (e.g., Palazzi et al., 2013; Ahmad et al., 2012; Krishnamurti and Kishtawal, 2000; Wu and Zhang, 1998; Li and Yanali, 1996), and the western disturbances (WDs) bringing moisture from the Mediterranean and Caspian sea as an extra-tropical frontal system during winter and early spring (Filippi et al., 2014; Pal et al., 2014; Mayer et al., 2014; Treydte et al., 2006; Syed et al., 2006; Archer and Fowler, 2004; Archer, 2001; Singh et al., 1995). Seldom, relatively weak storms of East Asian summer monsoon (Ding and Chan, 2005; Wang and Lin, 2002) also enter into the Ladakh region from the eastern end.

The summer monsoon in the Indus basin, extending from July–September, is the northwestern limit of the ISM. There are three monsoon moisture trajectories: 1st from the Indian Ocean across the Arabian Sea, 2nd along the Indian river valley to the western Himalayas and TP, and 3rd from the Bay of Bengal moving northward to the eastern Himalayas and TP along the Brahmaputra river valley (Pang et al., 2014; Liu, 1989; Lin and Wu, 1990). The WDs enter the north-west Indus basin during late November mostly in a diffused state with distorted structure, but regain their frontal structure and strength by interacting with the pre-existing orographically-maintained trough of low pressure. They usually bifurcate into the northern and southern branches around the Karakoram and western TP regions due to topographic blocking (Pang et al., 2014). Wintertime precipitation in the HKH region is mainly related to water vapour transport by the southern branch of WDs (Yihui and Zunya, 2008; Wei and Gasse, 1999). The interplay between these regional-scale atmospheric circulation systems and the local climatic and topographic features usually determine the amount and distribution

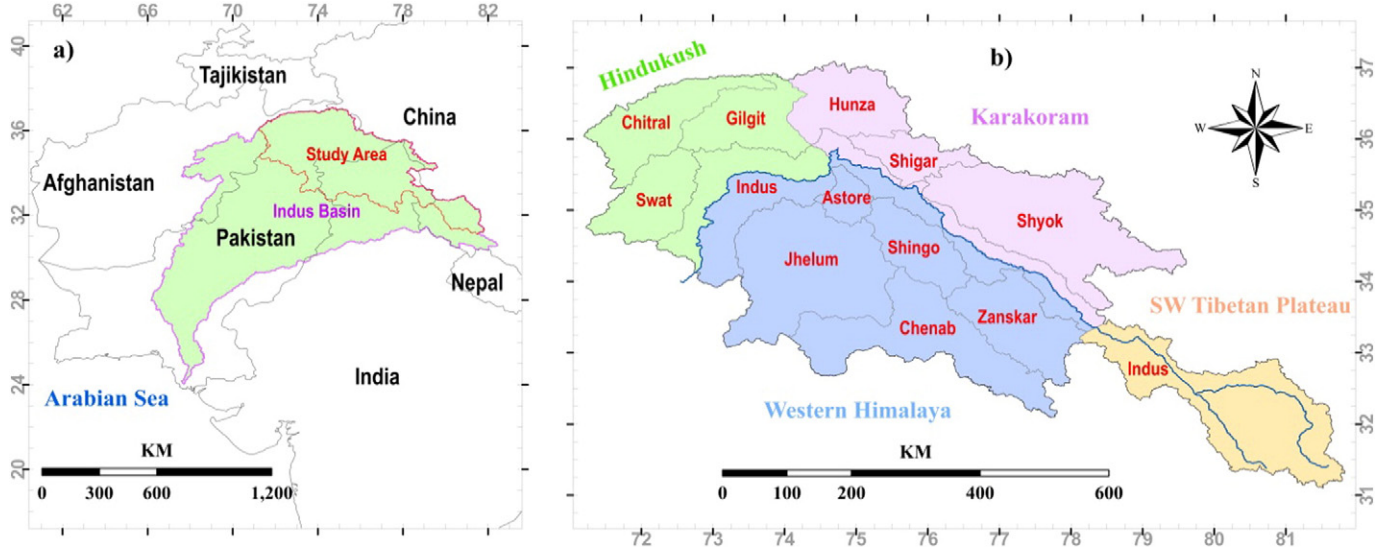

Fig. 1. a) Location of the study area, and b) location of sub-basins and mountain ranges. The mountain ranges of Hindukush, Karakoram, Western Himalaya and South-west TP are separated by different colour schemes.

pattern of precipitation in the high-altitude catchments of Indus basin.

3. Data and methods

3.1. Station based point observations

Meteorological data of the Indus basin is scattered among different organizations [e.g. Pakistan Meteorological Department (PMD), Water and Power Development Authority (WAPDA) of Pakistan, Indian Meteorological Department (IMD), University of Boon under the Culture Areas Karakoram (CAK) programme in the Bagrot valley and Yasin catchment of Gilgit basin during 1990–91, and Ev-K2-CNR (an Italian based organization) under the SHARE project]. However, not all these data are freely accessible. PMD operates a number of meteorological stations in Pakistan but their network of observatories in the high-altitude catchments of Indus basin is sparse and mainly concentrated in the valleys with elevations less than 2500 m a.s.l. WAPDA installed a network of meteorological observatories in various sub-basins of Indus basin under the Surface Water Hydrology Project and more recently (1994–99) under the Snow and Ice Hydrology Project mainly at the higher altitudes. We collected climatic data of 21 stations from PMD and 44 stations from WAPDA located in the study area. Monthly summaries of the observed precipitation at 41 observatories located in the Indian Territory available from NOAA-NCDC's website http://www.ncdc.noaa.gov/cdo-web/datasets (NOAA-NCDC) were downloaded in June, 2014. Meteorological data of 2 observatories installed by Ev-K2-CNR in Shigar basin were downloaded from http://data.eol.ucar.edu/codiac/dss/id?76.200 in June, 2014. The meteorological data collected under the CAK project in Gilgit and Hunza basins are not publicly available therefore we derived average precipitation of 10 observatories from Winiger et al. (2005), Miehe et al. (2001, 1996) and Eberhardt et al. (2007). Finally, we assumed 16 virtual stations located at the accumulation zones of major glaciers where average annual net precipitation is estimated from mass balance studies (Table 1). The observed station data used in this study are shown in Fig. 2 and further detailed in Appendix A.

3.2. Gridded datasets

Substantial progress has been made during the last three decades in constructing the analysed fields of precipitation over global land areas from multiple sources. As such, a wide variety of global and/or regional scale gridded precipitation products derived through various means is currently available for climate change and hydrological assessment studies. The most common and widely used products can broadly be classified into four categories; (i) based on climate models' reanalysis, (ii) merged model (reanalysis) and station observations, (iii) merged satellite estimates and station observations, and (iv) derived solely from station observations. In this study, we have selected at least one dataset from each basic category to underline the inherent errors associated with these datasets and highlight the importance of their bias correction before use in hydro-climate studies in the study area.

3.2.1. ERA-Interim

ERA-Interim (Dee et al., 2011) is a third generation global atmospheric reanalysis product with an improved atmospheric model and assimilation system, produced by the European Centre for Medium-range Weather Forecasts (ECMWF) providing data from 1979 to present. Estimates of precipitation associated with the reanalysis are produced by the forecast model, based on temperature and humidity information derived from assimilated observations. These data are available at sub-daily, daily and monthly intervals and at spatial resolution of 0.75° latitude–longitude grid, but we used monthly means of daily means re-gridded at 0.125° available at http://apps.ecmwf.int/datasets/data/interim-full-moda/, accessed in January, 2015. Berrisford et al. (2011) provides a detailed description of the ERA-Interim product.

3.2.2. WFDEI

The WATCH Forcing Data-ERA Interim (WFDEI) dataset (Weedon et al., 2014) is derived from ERA-Interim reanalysis product (Dee et al., 2011) via sequential interpolation to a 0.5° resolution, elevation correction and monthly-scale adjustments based on CRU TS3.1/TS3.21 (Harris et al., 2013) and GPCCv5/v6 (Schneider et al., 2013) monthly precipitation observations for 1979–2012 combined with new corrections for varying atmospheric aerosol-loading and separate precipitation gauge corrections for rainfall and snowfall under the Water and Global Change (WATCH) programme of the European Union. The WFDEI is an open access dataset at ftp://rfdata:forceDATA@ftp.iiasa.ac.at/. We accessed the data in December, 2014 and used CRU TS3.1/TS3.21 adjusted WFDEI product.

3.2.3. TRMM

The Tropical Rainfall Measuring Mission (TRMM), launched in November 1997 as a joint project by NASA and the Japanese Space Agency (JAXA), is instrumented with Precipitation Radar (PR), TRMM Microwave Imager (TMI), and Visible Infrared Scanner (VIRS). The PR provides three-dimensional maps of storm structure giving information on the intensity, distribution and type of rain, storm depth and the height at which the snow melts into rain. The TMI quantifies water vapour and cloud water content as well as the rainfall intensity in the

Table 1
Net annual precipitation as water equivalent (we) at the major glacier accumulation zones.

Sr. no.	Virtual station	Latitude (dd)	Longitude (dd)	Altitude (m)	we (mm)	Data source
1	Sentik	33.996667	75.95000	4908	620	Mayewski et al. (1984)
2	Nun Kun North	34.121927	76.10142	5200	900	Mayewski et al. (1983) and Qazi (1973)
3	Batura	36.666667	74.38333	4840	1034	Batura Investigation Group (1979)
4	Baltoro	35.877780	76.55079	5500	1600	Mayer et al. (2006) and Decheng (1978)
5	Urdok	35.766876	76.70253	5400	1060	Mayer et al. (2014)
6	Whaleback	36.057170	75.59149	4900	1790	Hewitt (2011, 2006) and Wake (1989)
7	Approach	36.067780	75.63310	5100	1880	Hewitt (2011, 2006) and Wake (1989)
8	Hispar East	35.849533	75.50639	4830	1070	Hewitt (2011, 2006) and Wake (1989)
9	Hispar Dome	36.010910	75.51872	5450	1620	Hewitt (2011, 2006) and Wake (1989)
10	Hispar Pass	36.028070	75.52151	5100	1420	Hewitt (2011, 2006)
11	Khurdopin	36.133770	75.61969	5520	2240	Hewitt (2011)
12	Nanga Parbat	35.167250	74.44442	4500	2000	Shroder et al. (2000) and Kick (1980)
13	Siachin A	35.470730	77.03757	4800	484	Bhutiyani (1999)
14	Siachin B	35.523490	76.99150	4950	526	Bhutiyani (1999)
15	Siachin C	35.518660	76.91160	5050	662	Bhutiyani (1999)
16	Siachin D	35.624230	76.85924	5350	855	Bhutiyani (1999)

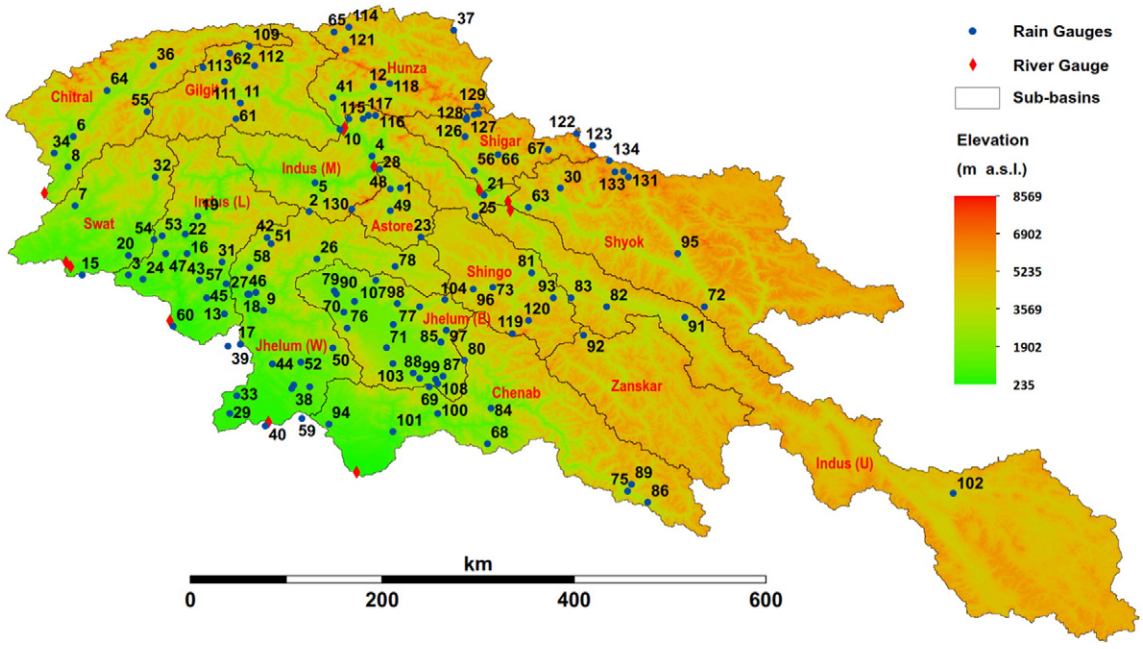

Fig. 2. Elevation distribution, sub-basins considered for altitudinal variation of precipitation, and location of rain gauges and river gauges (the numbers refer to the respective rain gauges mentioned in Appendix A).

atmosphere, while the VIRS provides the cloud context of the precipitation and connects microwave precipitation information to infrared-based precipitation estimates from geosynchronous satellites. The TRMM Multi-satellite Precipitation Analysis (TMPA) combines all the available precipitation datasets from different satellite sensors and monthly surface rain gauge data to provide a "best" estimate of precipitation at spatial resolution of 0.25° for the 50°N–S areas (Huffman et al., 2007). We used TRMM 3B43 version 7 monthly precipitation product released by TMPA in May 2012. Huffman et al. (2007) provide detailed information on the algorithms and different processing steps. The dataset available at http://disc.sci.gsfc.nasa.gov/daac-bin/DataHoldingsPDISC.pl?LOOKUPID_List=3B43 was accessed in December, 2014.

3.2.4. APHRODITE

Asian Precipitation-highly Resolved Observational Data Integration Towards Evaluation of Water Resources (APHRODITE) is the state-of-the-art high resolution daily precipitation dataset developed by a consortium between the Research Institute for Humanity and Nature (RIHN) Japan and the Meteorological Research Institute of Japan Meteorological Agency (MRI/JMA) from a dense rain gauge observational network in Asia. We used the latest and improved version of daily dataset for Monsoon Asia (APHRO_MA_V1101) covering 60.0E–150.0E, 15.0S–55.0N at a high spatial resolution of 0.25° for the period extending from 1951–2007 (Yatagai et al., 2012). The precipitation data from a dense network of rain gauges is 1st interpolated on to a grid of 0.05° using the modified version of the distance-weighting interpolation method (Shepard, 1968), which considers sphericity and orography by the Spheremap (Willmott et al. 1985) and the Mountain Mapper (Schaake, 2004) methods respectively. This dataset is then re-gridded to 0.25° and 0.5° products using the area-weighted mean. The algorithm is improved in that the weighting function considers the local topography between the rain-gauge and interpolated point (Yatagai et al., 2012). The very high resolution (0.05°) dataset is restricted to the partner institutes only and is not publicly available. Therefore, we used the latest and improved version of daily dataset for Monsoon Asia (APHRO_MA_V1101) covering 60.0E–150.0E, 15.0S–55.0N at a high spatial resolution of 0.25° for the period extending from 1951–2007 (Yatagai et al., 2012). The dataset, available at http://www.chikyu.ac.jp/precip/, was accessed in July, 2014.

3.3. River flow data

Historical daily discharge data at the sub-basin level for twelve stations (Fig. 2; Indus at Kharmong, Shyok at Yugo, Shigar at Shigar, Hunza at Dainyor, Gilgit at Gigit, Astore at Doyian, Indus at Tarbela, Chitral at Chitral, Swat at Chakdara and Zulam bridge — on Punjkora tributary, Jhelum at Mangla, and Chenab at Marala) in the study area are available from WAPDA. The current study uses river discharge data for the 1998–2012 period for consistency with the observed and gridded precipitation products.

3.4. Methods

The pre-processed void free Shuttle Radar Topography Mission (SRTM) digital elevation data of 90 m resolution freely available from http://hydrosheds.cr.usgs.gov/are used to delineate the watershed boundaries according to the methodology explained by Khan et al. (2014). However, for consistency with the precipitation datasets, the boundaries are also delineated from 1 km (30 s) DEM available from the same site.

We selected all the stations that covered at least three years of data to cover the recent installations and keeping in view the paucity of the observed data. Daily precipitation observations were converted into monthly totals if no more than three days were missing in a month. Similarly, seasonal and annual totals were calculated if no month was missing in a season or year. The study used station observations of average monthly, seasonal and annual precipitation totals from 134 points located within the study area to analyse altitudinal dependency and derive spatiotemporal distribution of precipitation averaged over the 1998–2012 period. In order to appraise the influence of elevation on precipitation, the average annual precipitation of a group of stations located within or closest to each sub-basin for the common time period are plotted.

For estimation of precipitation distribution, we selected the best suited spatial interpolation scheme based on literature review and specific geo-hydro-climatological conditions of our study area. While going

through the literature, we noticed that with wide and increasing applications of the spatial interpolation methods, there is also a growing concern about their accuracy and precision for a given set of conditions (Hartkamp et al., 1999). In general, when quality and amount of sampled data is sufficiently high, most of the spatial interpolation methods are accurate and produce almost similar estimates (Burrough and McDonnell, 1998). Minasny and McBratney (2007) however argued that improvements in prediction rely more on representativeness and quality of input data rather than on more sophisticated methods. A thorough review of spatial interpolation methods by Li and Heap (2014) could not infer any simple answer or consistent findings regarding the choice of best method, but it provided guidelines and suggestions by describing and comparing the features, strengths and weaknesses of a number of interpolators. Li and Heap (2011) analysed the performance of 32 spatial interpolation methods and observed that their performance depends not only on the structure of the method itself, but also on the nature of interpolating surface as well as quality and amount of the input data. They found kriging methods better than non-geostatistical methods and recommended Kriging with External Drift (KED) method. Many other studies (e.g. Tobin et al., 2011; Haberlandt, 2007; Verfaillie et al., 2006; ICES, 2005; Hengl et al., 2003; Rivoirard and Wieland, 2001; Bourennane et al., 2000; Bishop and McBratney, 2001; Goovaerts, 2000) also compared different geostatistical and non-geostatistical methods in a variety of situations and noticed that Kriging with KED usually provided better estimates than all other methods. The KED interpolation method (Schabenberger and Gotway, 2005) allows the processing of non-stationary random functions taking into account the spatial dependence of a primary variable known only at a small set of points as well as its linear relation to one or more additional covariates (secondary variables/predictors) exhaustively known at all points over the whole domain. It uses semivariograms or covariances, cross-covariance, transformations, trend removal, and allows for error/uncertainty check. It is most appropriate when there is an overriding trend in the sampled data, which can be modelled by a deterministic polynomial function. Moreover, Masson and Frei (2014) observed simple one-predictor KED model markedly better than the multilinear regression model with nine predictors and noticed only marginal improvement with the inclusion of complex physiographic predictors. Therefore, we selected KED interpolation method with elevation as a predictor to predict unknown values from these observations, as our study area is largely an under-sampled and complex high-mountain terrain exposed to three main circulation systems leading to reasonable spatial (directional) and altitudinal bias/trend in precipitation distribution.

The KED model includes a component of spatial autocorrelation and a component for multilinear dependence on pre-defined variables (predictors). It considers the observations ($\boldsymbol{Y}$) at sample locations ($\boldsymbol{s}$) as a random variable of the form (e.g. Diggle and Ribeiro, 2007):

$$\boldsymbol{Y}(\boldsymbol{s}) = \mu(\boldsymbol{s}) + \boldsymbol{Z}(\boldsymbol{s}) \quad (1)$$

$$\boldsymbol{\mu}(\boldsymbol{s}) = \beta_0 + \sum_{k=1}^{K} \boldsymbol{\beta_k} \cdot \boldsymbol{x_k}(\boldsymbol{s}) \quad (2)$$

Here, $\boldsymbol{\mu}(\boldsymbol{s})$ describes the deterministic component of the model (external drift or trend) and is given as a linear combination of $\boldsymbol{K}$ predictor fields $\boldsymbol{x_k}$ ($\boldsymbol{s}$) (trend variables) plus an intercept ($\boldsymbol{\beta_0}$). $\boldsymbol{\beta_k}$ is denoted as trend coefficients, while $\boldsymbol{Z}(\boldsymbol{s})$ describes the stochastic part of the KED model and represents a random Gaussian field with a zero mean and a 2nd order stationary covariance structure. The latter is conveniently modelled by an eligible parametric semi-variogram function describing the dependence of semi-variance as a function of lag (possibly with a directional dependence). To derive the climatology of mean monthly, seasonal and annual cycle of precipitation from the point observations, we applied KED interpolation method with elevation as a predictor separately for monthly, seasonal and annual precipitation totals averaged over the period of 1998–2012. The KED-based estimated precipitation distribution was further converted into grid format (1 km grid size) for computation of sub-basin scale precipitation and ultimate comparison with the gridded datasets.

Daily river discharge data from the available outlets (gauges) are used to compute the average monthly, seasonal and annual specific runoff (measured flow/drainage area) for each sub-basin. The KED-based estimated annual precipitation totals from each sub-hydrological basin are validated by the corresponding average specific runoff and the pattern of glacier cover using ICIMOD glacier inventory (Bajracharya and Shrestha, 2011) and compared with earlier studies.

The selected gridded precipitation products are re-gridded and processed to compute mean monthly, seasonal and annual precipitation totals at sub-basin scale. Afterwards, their accuracy relative to the KED-based estimated precipitation is evaluated for each sub-hydrological basin. For evaluation of precipitation patterns, the Taylor diagram is used for the re-gridded precipitation values of all the products to a common grid of 0.05°; while for quantitative assessment, the seasonal and annual biases relative to the KED-based estimated precipitation at the sub-basin scale are analysed. Basin-wide seasonal and annual correction factors are introduced to account for the inherent errors in each gridded product. These correction factors are determined by dividing the respective grid values of the estimated precipitation by the gridded datasets and averaging them at sub-basin level. For utilization, these factors simply need to be multiplied with the respective gridded datasets for the area of interest.

3.5. Uncertainty analysis

The major uncertainties involved in this study are associated with the quality and amount of the observed data and the interpolation technique used to predict the unknown values from these observations. The organizations operating weather stations in the study area generally indicate to apply WMO standards for collection of meteorological data. Yet, in many cases, the quality of data is affected by instrumental problems, station locality and interruption of time series (Miehe et al., 1996). PMD, WAPDA and Ev-K2-CNR use the tipping bucket rain gauges to record liquid precipitation in the low- to mid-altitude areas. In the case of occasional snowfall, the water equivalent calculated manually is usually added to the daily precipitation records. The automatic data collection platforms (DCPs) installed by WAPDA in the high-altitude areas during 1994–95 use snow pillows to measure both solid and liquid precipitation as water equivalent. However, most of the installed snow pillows encountered technical issues of interfacing with the transmission system as well as unexpected "jumps" due to possible ice bridging and rupture effects (SIHP, 1997). Although, the problem was substantially minimized in 1996 by attaching a precision potentiometer to convert the shaft encoders from a digital output to an analogue, the snow pillows are still subjected to underestimate solid precipitation under strong wind conditions (Hasson et al., 2014). The automatic weather stations installed within the framework of the CAK project measure precipitation using data logger, tipping bucket and snow depth gauge (Miehe et al., 1996). Yet, measurement of solid precipitation in strong windy conditions is subject to considerable errors due to constant blowing away of snow from the ultrasonic sensors. GHCN-monthly summaries of the observed precipitation for the study area are based on data from IMD, which also follows WMO standards, and are subjected to a suite of quality assurance reviews.

Another source of uncertainty is inconsistency in the precipitation observations due to late installation of instruments, temporary sensor failures or non-collection of data. The time series of the observed data is variable, ranging from more than 30 years for a few stations to at least 3 years for the most recently installed stations (Appendix A). We used average precipitation during the period of 1998–2012, because majority of data is available for this period except the GHCN dataset, which contains precipitation data of some old observatories operational between 1901 and 1970. To check for possible temporal change, we

compared these stations' records with the nearest stations with up to date data. We only found an insignificant trend. Similarly, the net precipitation estimated from glacier accumulation studies is also inconsistent in temporal terms.

KED interpolation model produces both prediction as well as error/uncertainty surfaces, giving an indication or measure of how good the predictions are. It estimates an interpolated surface from randomly varied small set of measured points and recalculates estimated values for these measured points to validate the estimates and determine extent of errors. Since, we used all of the available observations; there is no more ground truth available to validate the performance of this method. However, we used leave-one-out cross validation strategy to assess the performance of the employed interpolation scheme. We applied cross validation on the observed and predicted values from all the stations to assess the errors/uncertainty associated with the interpolation scheme by using error scores of the relative bias (B) and the relative mean root-transformed error (E), which are defined as:

$$\boldsymbol{B} = \frac{\sum_{i=1}^{n} \boldsymbol{P_i}}{\sum_{i=1}^{n} \boldsymbol{O_i}} \tag{3}$$

$$\boldsymbol{E} = \frac{\frac{1}{n}\sum_{i=1}^{n}\left(\sqrt{\boldsymbol{P_i}} - \sqrt{\boldsymbol{O_i}}\right)^2}{\frac{1}{n}\sum_{i=1}^{n}\left(\sqrt{\boldsymbol{O}} - \sqrt{\boldsymbol{O_i}}\right)^2}. \tag{4}$$

Here $\boldsymbol{P_i}$ and $\boldsymbol{O_i}$ are the predicted and observed precipitation values respectively, while $\boldsymbol{O}$ is the spatial average of the observations over all (or a subset of n) stations. The cross validation results (Table 2) depict relative bias values of slightly higher than for all months, indicating only a small overestimation of the predicted values but at annual scale it is almost zero. Similarly, E values less than 1 suggest typical errors smaller than the spatial variations except for pre-monsoon season. In summary, there are no serious uncertainties or constraints but further improvements in the estimated precipitation distribution can be achieved by using higher quality observed data with more spatiotemporal coverage, particularly at higher-altitudes.

4. Results

4.1. Altitudinal variation of precipitation

The analysis of observed precipitation records revealed significant altitude dependency of precipitation in all the sub-basins (Fig. 3), which supports earlier studies (e.g. Pang et al., 2014; Winiger et al., 2005; Hewitt, 2011; Weiers, 1995; Wake, 1989; Dhar and Rakhecha, 1981; BIG, 1979; Decheng, 1978). However, there is substantial difference in the rate and magnitude of variation from one basin to another due to significant directional bias (spatial autocorrelation) and influence of highly diversified orography (topography and exposure) interacting with multiple weather systems. Therefore, the complex altitudinal variation of precipitation in the high-altitude Indus basin cannot be represented by a single relation. Such an elusive behaviour of precipitation gradient was also found by Immerzeel et al. (2014) in Nepalese Himalayas, where a uniform valley wide precipitation gradient could not be established due to influence of several scale-dependent mechanisms. Although, we attempted a separate analysis for each sub-hydrological basin, yet the spatial variability in each sub hydrological basin is so high that the number of available observations is inadequate to infer an accurate distribution of altitudinal precipitation. Rather complex and nonlinear trend of precipitation increase with altitude is evident in most sub-basins. The south-west TP and eastern Karakoram regions display an elusive trend mainly due to higher variability and very less number of observation points. Astore and Chitral basins depict mixed trend, while Shigar, Hunza and Gilgit basins infer relatively strong positive vertical gradients. The southern basins like Chenab, Jhelum, Swat and

Table 2
Relative bias (B) and relative mean root-transformed error (E) calculated over all observation points. PMSN is pre-monsoon (Apr–Jun), MSN is monsoon (Jul–Sep), WIN is winter (Oct–Mar) and ANN is annual.

	Jan	Feb	Mar	Apr	May	Jun	Jul	Aug	Sep	Oct	Nov	Dec	PMSN	MSN	WIN	ANN
B	1.014	1.029	1.040	1.045	1.045	1.015	1.002	1.004	1.002	1.005	1.005	1.036	1.043	1.002	1.003	1.001
E	0.090	0.786	0.913	1.189	1.858	1.007	0.003	0.009	0.022	0.012	0.055	0.935	1.406	0.006	0.011	0.006

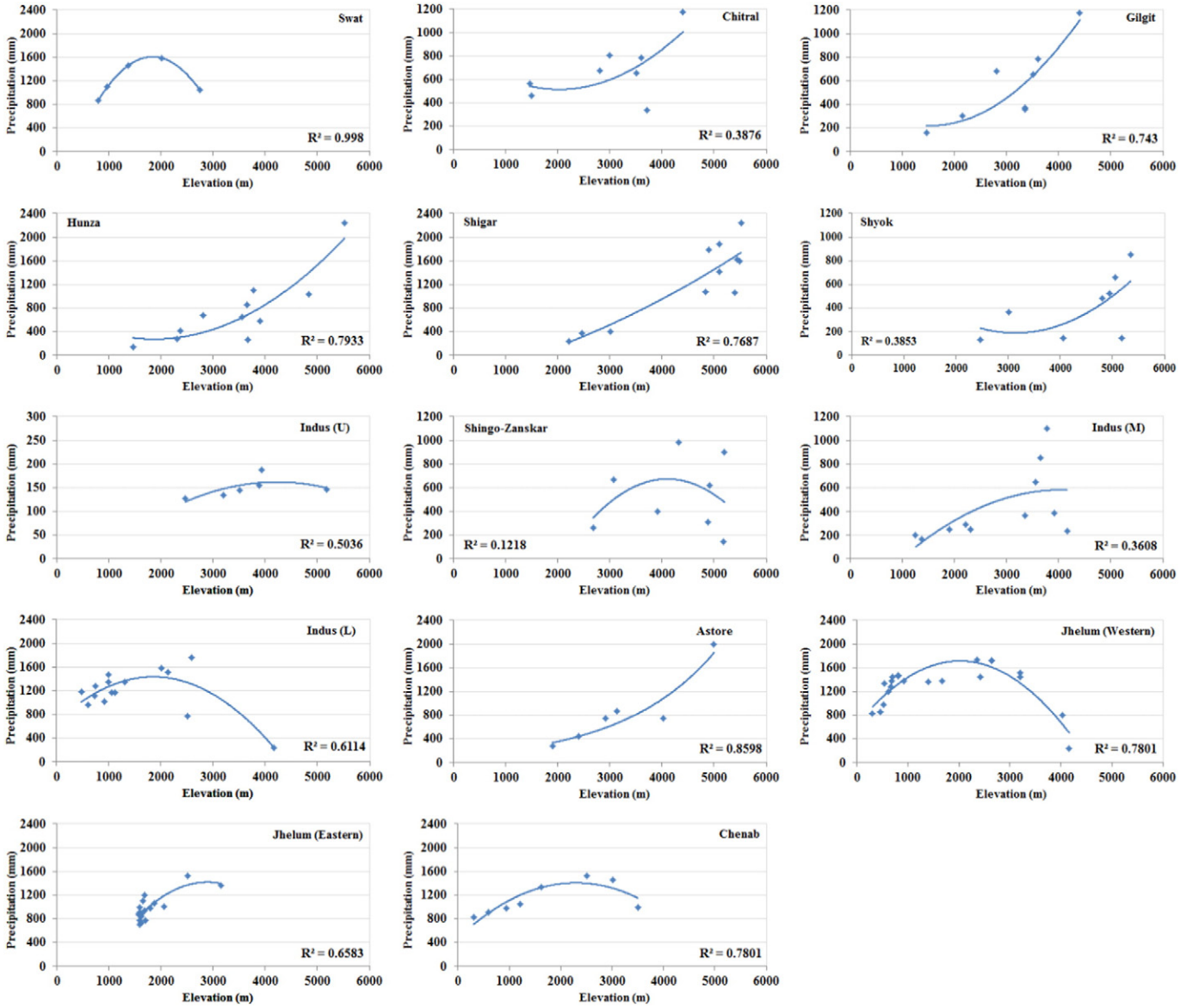

Fig. 3. Altitudinal variation of annual precipitation in each sub-basin.

Lower most reach of Indus main experience the zone of maximum precipitation at an altitude of around 2500 m. Pang et al. (2014) and Dhar and Rakhecha (1981) also observed that the monsoon precipitation above 2400 m elevation in the central Himalayas decreases significantly with rising elevation. The height of maximum precipitation in rest of the sub-basins is not clear but tends to increase with latitude. Hence, the assumptions of linear increase in precipitation with elevation by the earlier studies (e.g. Immerzeel et al., 2012; Mayer et al., 2006 and Winiger et al., 2005) could not be confirmed by this study as the available observations are highly inadequate to infer an accurate distribution of altitudinal precipitation.

4.2. Spatial interpolation of precipitation observations

The KED-based interpolation of the point observations revealed some important characteristics of precipitation distribution in the study area. Monthly distribution of precipitation indicates largely bimodal weather system in the study area reflecting the wintertime precipitation associated with the westerly systems and the impact of Indian summer monsoon. The south-western Himalayan catchments (Chenab, Jhelum and Indus-L) are dominated by the summer monsoon but also receive considerable amounts of precipitation during winter and pre-monsoon seasons. The Hindukush and Karakoram basins receive most of their precipitation during winter (40–60%) and pre-monsoon (25–45%) seasons. The winter precipitation usually strengthens in December, peaks in March and starts receding during April and is very important for accumulated summer flows particularly in the Hindukush and Karakoram regions (Fig. 4).

The hydrographs of estimated precipitation and specific runoff (Fig. 4) indicate dominancy of snow/glacier melt contribution during May–September. Since, snowfields and glaciers often perform an important function of regulating stream flows, the downstream areas usually receive heavy floods whenever higher precipitation in winter season is followed by a relatively warm and wet monsoon season. Due to varying inputs of precipitation and snowmelt components, there is large variability in the amount (depth) of peak flows from different sub-basins but the timing tends to be in late July for most of the basins. Generally, the river flows are very low during winter, start rising in May, peak in July–August and descend sharply until the start of next winter. The high-altitude western and northern basins (Chitral, Gilgit, Hunza,

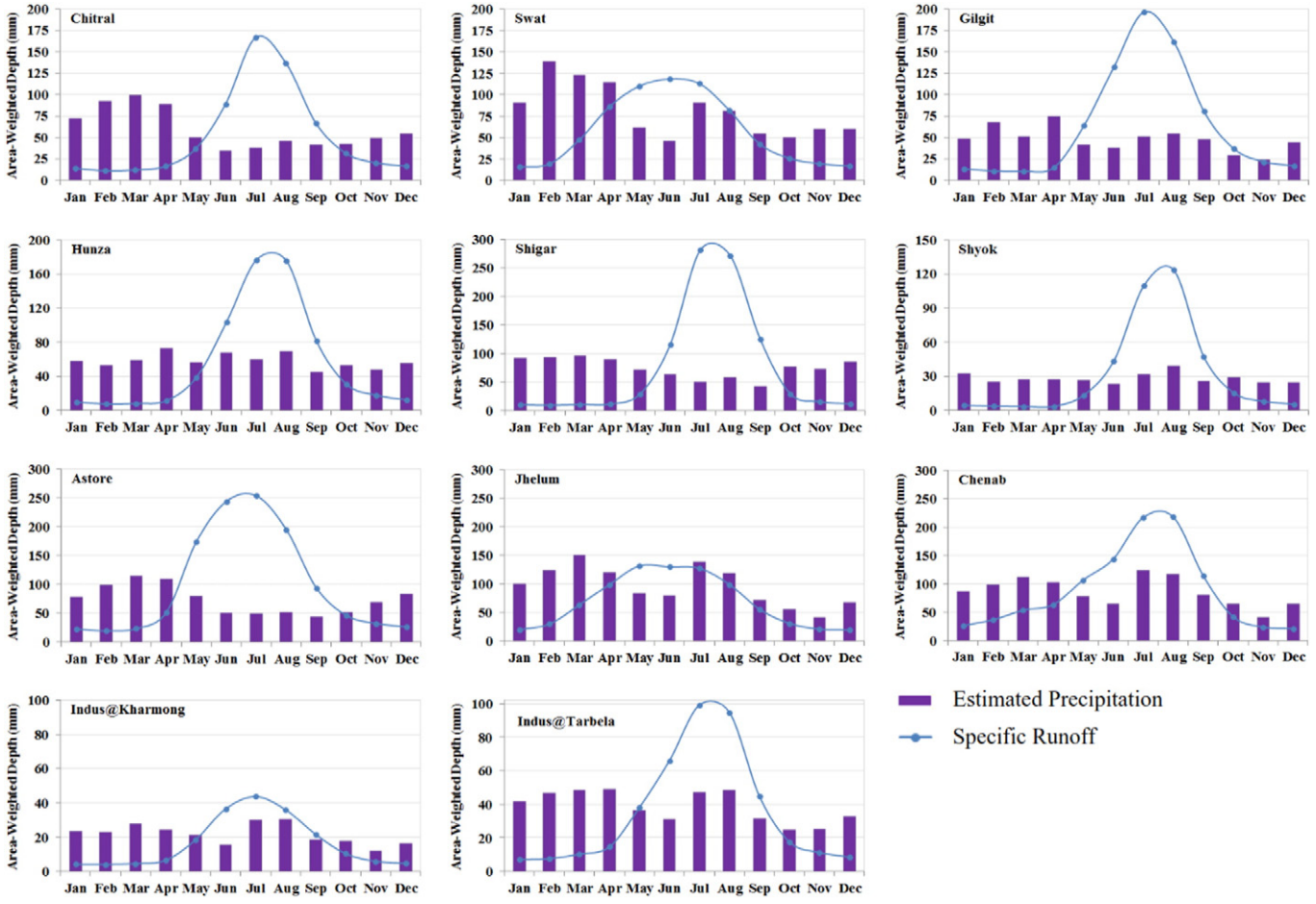

Fig. 4. Monthly distribution of basin wise area-weighted depths of estimated precipitation and specific runoff.

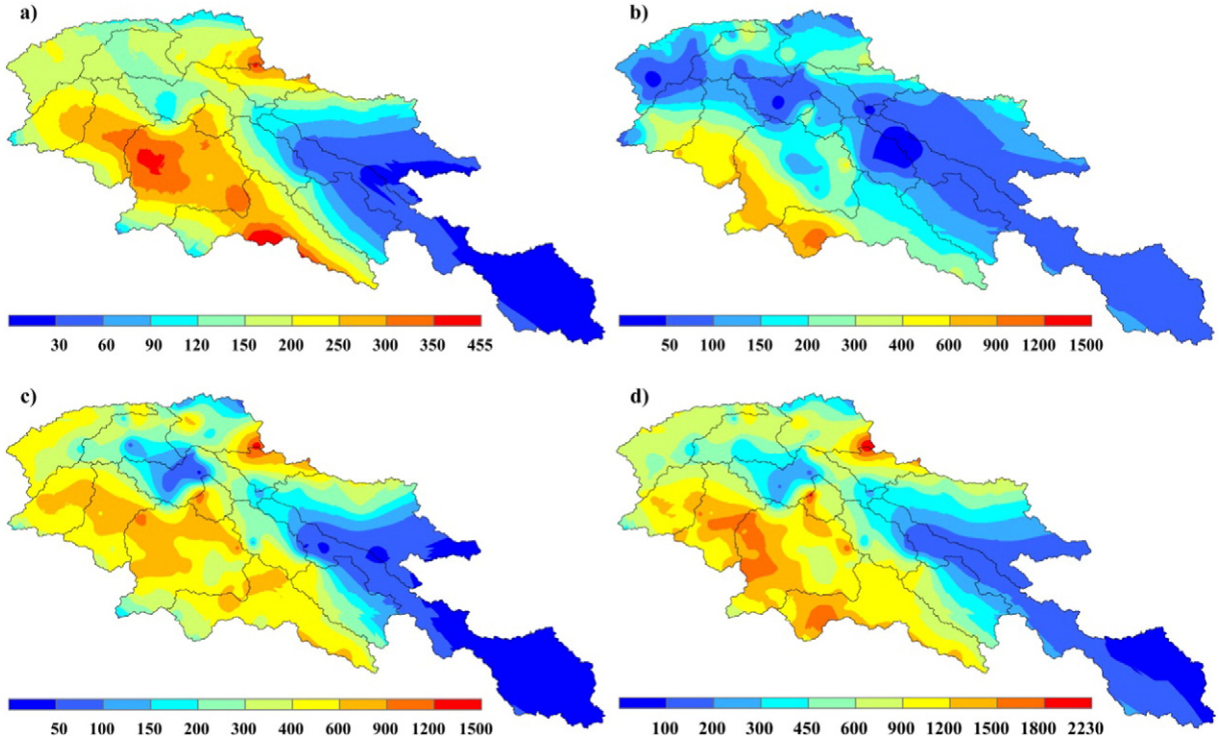

Fig. 5. Spatial distribution of KED based estimated precipitation for a) pre-monsoon (Apr–Jun), b) monsoon (Jul–Sep), c) winter (Oct–Mar) and d) annual basis. All values are in mm (note different scales for each panel).

Shigar, Shyok, Indus at Kharmong and Astore) are more dominated by snow/glacier melt while the low-altitude southern basins (Swat, Indus-lower, Jhelum and Chenab) receive substantial flows from direct rainfall.

The estimated precipitation distribution (Figs. 4 and 5) signifies the key features of mean annual cycle and seasonality of precipitation. Moisture-laden westerly winds are intercepted by high mountains in the west and north, leading to moisture condensation and precipitation at higher altitudes. As such, winter precipitation tends to be stronger in Chitral, Swat, Gilgit, Hunza, Astore and Shigar basins, which receive significant precipitation in the form of snowfall during winter and spring (pre-monsoon) seasons. The Indian summer monsoon mainly dominates at southern parts (i.e. Chenab, Jhelum, Swat and Indus-lower basins). Northwardly oriented Astore, Shingo and Zanskar basins are on the leeward side of western Himalayan range and thus receive lower precipitation as compared to Chenab and Jhelum basins in monsoon season. The Tashain glacier and Nanga Parbat massif located in the south-west of Astore basin hinder further north-west movement of the monsoon. However, stronger storms often divert northwardly and penetrate in to the central Karakoram region. Highly elevated boundary between Chenab and Zanskar basins hardly allows monsoon rains to penetrate further northward; as such the Zanskar range and Ladakh region in the TP are relatively drier. The East Asian summer monsoon seldom reaches to the Karakoram from the east. However, whenever it does penetrate significantly, it interacts dramatically with the features of the already present Indian summer monsoon and westerly systems causing heavy downpours and extensive floods (e.g. Jul–Aug 2010 floods in Pakistan). The Indus main up to Chilas (climatic station number 5 in Fig. 2), which remains under the rain shadow of the surrounding high mountains on both sides, is least affected by both summer monsoon and western disturbances.

4.3. Validation of KED-based estimated precipitation

The basin-wide KED-based estimated precipitation is validated by the specific runoff (measured flow/drainage area) of respective sub-basins (Fig. 6a). The specific runoff in snow/glacier fed basins is usually affected by precipitation losses and the dynamics of snow/glacier mass balance as the river flows are often regulated by changes in storage of snow/glacier mass. In the absence of comprehensive and reliable mass balance estimates, the estimated precipitation and the corresponding specific runoffs can be used to infer the change in snow/glacial mass balance. Positive changes in storage are expected when the net precipitation (excluding losses) is markedly greater than river runoff. Conversely, higher runoff compared to the net precipitation may point to loss of storage indicating negative mass balance. However, reliable estimates on evapotranspiration, interception, sublimation and percolation losses in the study area are lacking, forcing earlier studies (e.g. Immerzeel et al., 2009; Tahir et al., 2011) to ignore these losses. The assumption that these components in water balance studies may be negligible particularly in the Karakoram region are supported by the fact that the majority of the landscape in this region is rocky with scarce vegetative cover resulting in minor evapotranspiration, interception and percolation. Nevertheless, these losses will result in reduced net precipitation. We used net precipitation from the glacier accumulation zones, which already excludes the losses from snowfields and glaciated areas. Moreover, there may be some compensating errors because the solid precipitation in the high-altitude and windy areas is generally susceptible to undercatch by 20–50% (Rasmussen et al., 2012). Therefore, we assume that the potential losses (evapotranspiration, sublimation, interception and deep percolation) and possible gains (undercatch of snowfall) cancel each other out and the net difference is insignificant particularly in the Karakoram and north-west Hindukush regions. Another approximation to validate the estimated precipitation is superimposition of glacier cover over the estimated precipitation (Fig. 6b) since an adequate amount of precipitation is essential to sustain and surge the glaciers in this area. The estimated precipitation coherently follows the pattern of glacier cover in high-altitude areas except the eastern Shyok basin.

Finally, the KED-based estimated precipitation is compared with the estimates of earlier studies derived either from station observations or gridded datasets. The comparative analysis, summarized in Table 3, shows that the precipitation estimates by earlier studies are highly contrasting but consistent in underestimating precipitation in majority of the areas. These earlier studies have used non-representative precipitation data and/or overestimated basin boundaries resulting in highly biased precipitation estimates.

4.4. Evaluation of the gridded products

The gridded precipitation products often fail to capture the large and abrupt changes in precipitation over short distances due to their coarse resolution and pronounced orographic effects in the high mountain areas. In this study, we evaluated accuracy of important precipitation products derived through four different means for the high-altitude areas of Indus basin. The spatial distribution of mean seasonal and annual precipitation totals from ERA-Interim, WFDEI, TRMM and APHRODITE products show contrasting timings and amplitudes (Table 4) and patterns (Fig. 7) relative to the KED-based estimated precipitation. In quantitative terms, ERA-Interim largely overestimates precipitation in all the sub-basins except Shigar and Hunza, while the other three datasets consistently underestimate precipitation in all the areas barring Ladakh region of the TP (Indus at Kharmong). However, the inter-comparison of the four gridded products show a reasonable consistency between TRMM and APHRODITE, while WFDEI tend to be slightly different and ERA-Interim displays large overestimates. Within the ambit of overall dry bias, WFDEI gives relatively better quantitative estimates for Hindukush, Karakoram and north-western Himalayan regions but

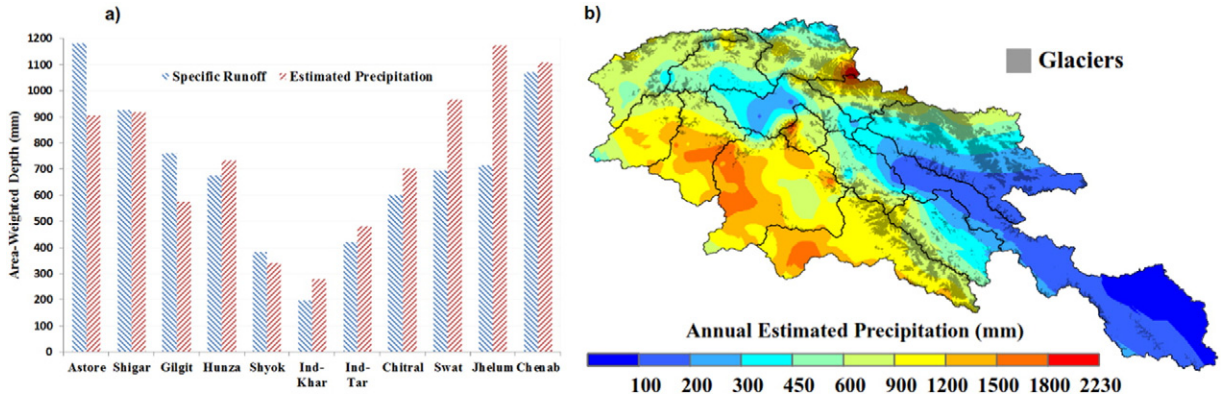

Fig. 6. Validation of KED-based estimated precipitation a) with specific runoff, and b) with glacier cover.

Table 3
Comparison of KED-based estimated precipitation with the estimates of earlier studies.

River basin	Precipitation (mm)	Dataset used	Reference study
Indus-Kharmong	388.0	Terrestrial Precipitation V2.01 (Matsuura & Willmott, 2009)	Mukhopadhyay (2012)
	277.3	Station data + KED interpolation	This study
	161.0	APHRODITE * 1.17	Lutz et al. (2014a)
Shyok	341.5	Station data + KED interpolation	This study
	251.2	Terrestrial Precipitation V2.01 (Matsuura & Willmott, 2009)	Mukhopadhyay (2012)
	175.5	APHRODITE * 1.17	Lutz et al. (2014a)
Shigar	917.2	Station data + KED interpolation	This study
	882.0	India-WRIS	CWC and NRSC (2014)
	550.0	Model	Bocchiola et al. (2011)
	264.0	APHRODITE * 1.17	Lutz et al. (2014a)
	201.7	Terrestrial Precipitation V2.01 (Matsuura & Willmott, 2009)	Mukhopadhyay (2012)
Hunza	828.0	Glaciers as proxy & station data	Immerzeel et al. (2012)
	732.8	Station data + KED interpolation	This study
	692.0	APHRODITE + Glacier as proxy	Lutz et al. (2014b)
	582.6	India-WRIS	CWC and NRSC (2014)
	229.7	Terrestrial Precipitation V2.01 (Matsuura & Willmott, 2009)	Mukhopadhyay (2012)
	205.0	APHRODITE * 1.17	Lutz et al. (2014a)
	176.0	APHRODITE	Tahir et al. (2011)
	162.5	Station observations	Akhtar et al. (2008)
Gilgit	582.6	India-WRIS	CWC and NRSC (2014)
	575.4	Station data + KED interpolation	This study
	326.0	APHRODITE * 1.17	Lutz et al. (2014a)
	315.0	Terrestrial Precipitation V2.01 (Matsuura & Willmott, 2009)	Mukhopadhyay (2012)
	162.5	Station observations	Akhtar et al. (2008)
Astore	904.6	Station data + KED interpolation	This study
	882.0	India-WRIS	CWC and NRSC (2014)
	496.0	Station observations	Akhtar et al. (2008)
	430.5	APHRODITE * 1.17	Lutz et al. (2014a)
Indus-Tarbela	675.0	ERA-Interim, NCEP/NCAR	Reggiani and Rientjes (2015)
	671.0	APHRODITE + Glacier as proxy	Lutz et al. (2014b)
	481.6	Station data + KED interpolation	This study
	315.0	Terrestrial Precipitation V2.01 (Matsuura & Willmott, 2009)	Mukhopadhyay (2012)
	311.0	TRMM 3B43	Immerzeel et al. (2009, 2010)
	300.0	TRMM 2B31	Bookhagen and Burbank (2010)
	218.9	APHRODITE * 1.17	Lutz et al. (2014a)
Jhelum	1175.2	Station data + KED interpolation	This study
	1052.5	India-WRIS	CWC and NRSC (2014)
Chenab	1333.8	India-WRIS	CWC and NRSC (2014)
	1107.5	Station data + KED interpolation	This study

seems less accurate for the south-western Himalaya, whereas TRMM shows opposite estimates for these areas. Similarly, TRMM gives better estimates during monsoon but WFDEI is better for the other seasons. The APHRODITE product is the least accurate among the four datasets showing strong dry bias for almost all seasons and all areas, particularly for winter and in the high-altitude catchments.

The pattern statistics of the mean annual precipitation in the study area (Fig. 8) show normalized RMSE values ranging from 0.6 for APHRODITE to 0.62 for TRMM, 0.72 for WFDEI and 0.8 for ERA-Interim product. The APHRODITE and TRMM products show a relatively higher correlation coefficient of around 80% against 73% by ERA-Interim and WFDEI products. It is important to note that these statistics only evaluate the pattern of the gridded datasets.

Overall, there is significant spatial (basin to basin) as well as temporal (season to annual) bias in the precipitation totals from all the four gridded datasets (Fig. 9). ERA-Interim largely displays positive bias

Table 4
Basin-wise mean seasonal and annual precipitation totals (mm) from estimated (EST), ERA-Interim (ERAI), WFDEI (WEI), TRMM (TRM), and APHRODITE (APH) precipitation products during 1998–2012.

River basin	Pre-monsoon					Monsoon					Winter					Annual				
	EST	ERAI	WEI	TRM	APH	EST	ERAI	WEI	TRM	APH	EST	ERAI	WEI	TRM	APH	EST	ERAI	WEI	TRM	APH
Indus-U	29.2	129.5	79.8	56.6	33.0	69.4	206.2	128.2	124.7	81.9	46.4	112.1	124.6	90.8	41.9	145.0	447.8	332.6	272.1	156.8
Zanskar	92.6	247.7	92.7	84.2	53.3	126.8	191.7	132.8	146.8	80.7	254.8	339.5	147.5	131.3	87.5	474.2	778.9	373.0	362.3	221.5
Shingo	135.1	281.3	110.3	121.1	78.3	98.0	174.1	117.2	119.3	58.1	322.6	516.6	208.3	190.8	115.7	555.7	972.0	435.8	431.2	252.1
Shyok	77.0	148.4	59.4	59.6	40.2	100.1	116.8	27.3	79.1	41.2	164.4	157.3	143.0	69.3	56.8	341.5	422.5	229.7	208.0	138.2
Shigar	224.7	206.8	88.5	67.6	90.8	160.4	120.9	31.7	101.8	46.8	532.2	318.5	202.1	117.2	87.9	917.2	646.2	322.3	286.6	225.5
Hunza	198.6	251.6	92.4	84.9	70.6	188.6	177.3	26.4	115.1	46.1	345.6	308.3	208.2	156.1	59.0	732.8	737.3	327.0	356.1	175.7
Gilgit	156.2	371.7	133.7	97.8	133.2	162.2	234.1	86.3	109.5	61.6	257.0	559.8	286.8	117.1	83.4	575.4	1165.6	506.8	324.4	278.2
Astore	235.5	352.1	124.6	129.7	135.6	153.0	262.1	116.6	138.8	64.3	516.2	590.7	241.1	173.1	134.5	904.6	1204.9	482.3	441.6	334.4
Indus-M	151.9	362.6	127.9	94.4	117.6	101.5	295.2	111.8	119.2	53.9	199.4	557.6	241.9	109.9	89.8	452.9	1215.5	481.6	323.5	261.3
Indus-L	237.6	343.1	22.7	187.2	214.9	355.8	662.4	330.1	347.3	338.2	542.9	620.0	368.9	306.8	364.0	1136.3	1625.6	721.6	841.3	917.1
Ind@Tar	115.7	228.0	102.2	86.0	77.7	133.1	231.6	109.6	134.6	86.9	232.9	317.7	191.8	127.6	94.9	481.6	777.3	403.6	348.2	259.5
Chitral	173.2	344.4	168.2	104.2	141.9	124.8	145.2	104.9	94.6	54.3	404.4	595.1	371.9	218.6	184.2	702.3	1084.7	645.0	417.4	380.4
Swat	218.5	332.1	218.5	172.8	200.3	224.9	620.5	250.1	234.6	222.6	522.7	655.7	393.6	368.7	415.7	966.1	1608.4	862.2	776.1	838.6
Jhelum	278.5	314.8	181.5	211.9	179.5	337.6	496.6	329.2	370.0	252.1	559.0	641.2	295.8	367.4	333.0	1175.2	1452.6	806.5	949.3	764.6
Chenab	242.4	289.9	140.1	162.7	137.5	353.6	401.6	303.3	427.1	272.6	511.6	563.4	198.5	290.8	288.3	1107.5	1254.9	641.9	880.6	698.4

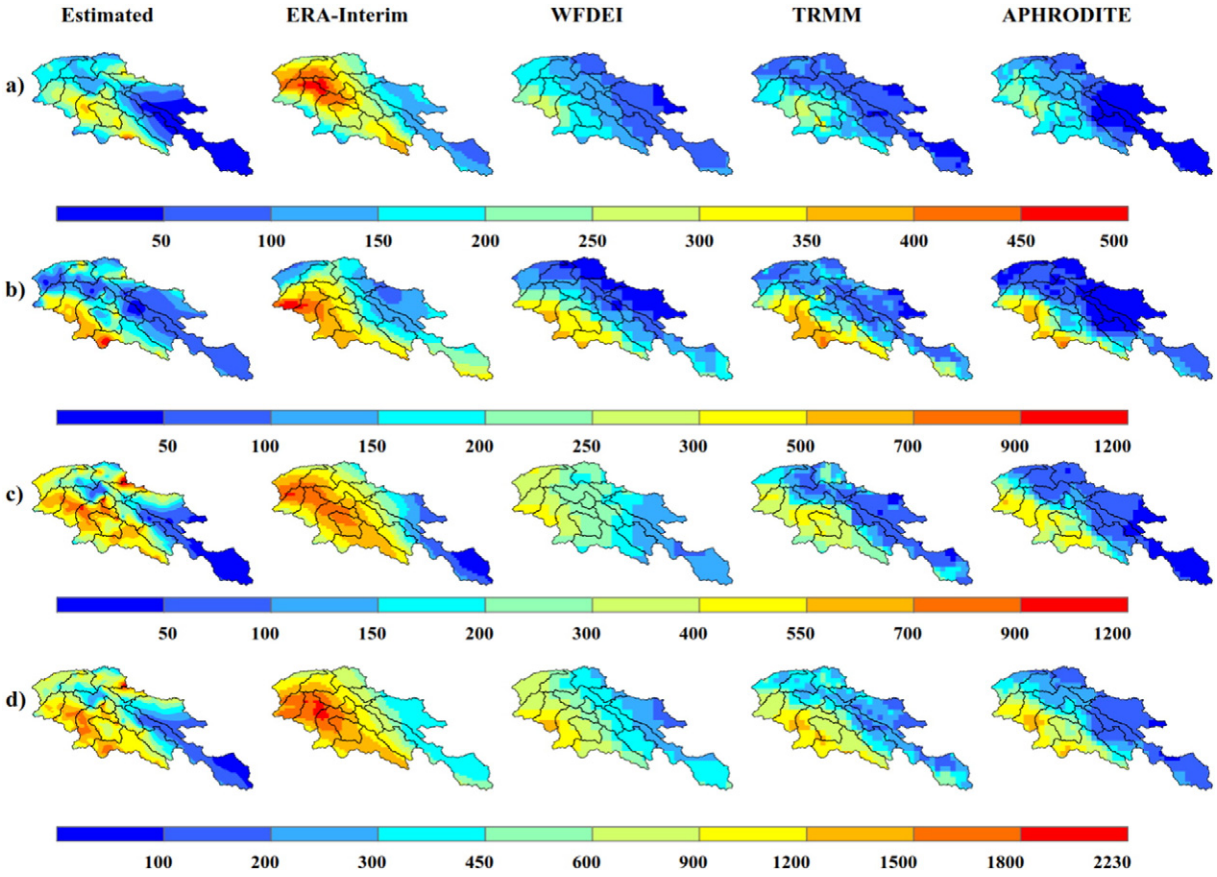

Fig. 7. Spatial distribution of mean precipitation by the estimated, ERA-Interim, WFDEI, TRMM and APHRODITE datasets for a) pre-monsoon, b) monsoon, c) winter, and d) annual basis. All values are in mm (note the different colour scales).

(overestimation) while the other three datasets show substantial negative bias (underestimation) in most parts of the study area. The highest negative bias is observed in the central Karakoram region consistently by all the datasets, whereas the positive bias is mainly concentrated in the Ladakh region. However, the estimated precipitation is very close to net precipitation, whereas the gridded precipitation products give gross precipitation amounts, which are subjected to some losses from precipitation. Hence, some room for overestimation can be permitted. Nevertheless, the extent of absolute bias suggests the importance of bias correction of the four gridded datasets before their use in hydro-climate studies in the study area. To support such a bias correction, we analysed the seasonal and annual biases relative to the estimated precipitation at the sub-basin scale and introduced appropriate correction factors to account for the inherent errors of each gridded dataset. These basin-wide seasonal or annual correction factors, summarized in Table 5, simply need to be multiplied with the respective gridded datasets for the area of interest. This will ensure reasonably well quantified estimates that can be used to avoid or minimize suboptimal calibration of model input parameters and compensation of one variable with another in the hydrological modelling and water balance studies.

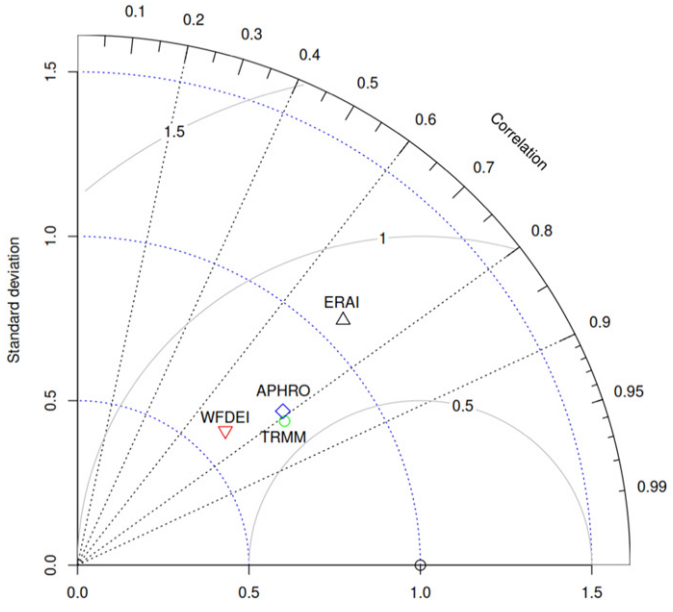

Fig. 8. Pattern statistics of mean annual precipitation in the study area for the four gridded products. The RMSE and standard deviations are normalized by those of the estimated precipitation.

5. Discussion

The altitudinal analysis of precipitation distribution demonstrates the typical orographic precipitation trend, which increases up to a certain height of maximum precipitation and thereafter decreases, in most of the sub-basins. However, the basin to basin difference in the rate and magnitude of change is considerable. These results are in good agreement with earlier studies for the Chenab basin (Arora et al., 2006 and Singh et al., 1995). The altitudinal dependency of precipitation expressed by the 2nd order polynomial functions indicates only the generalized trend of precipitation variation with altitude. The exact behaviour of precipitation is too complex to be represented by such functions. Presence of spatial autocorrelation and very high uncertainty beyond the altitudinal extent of the point observations, particularly

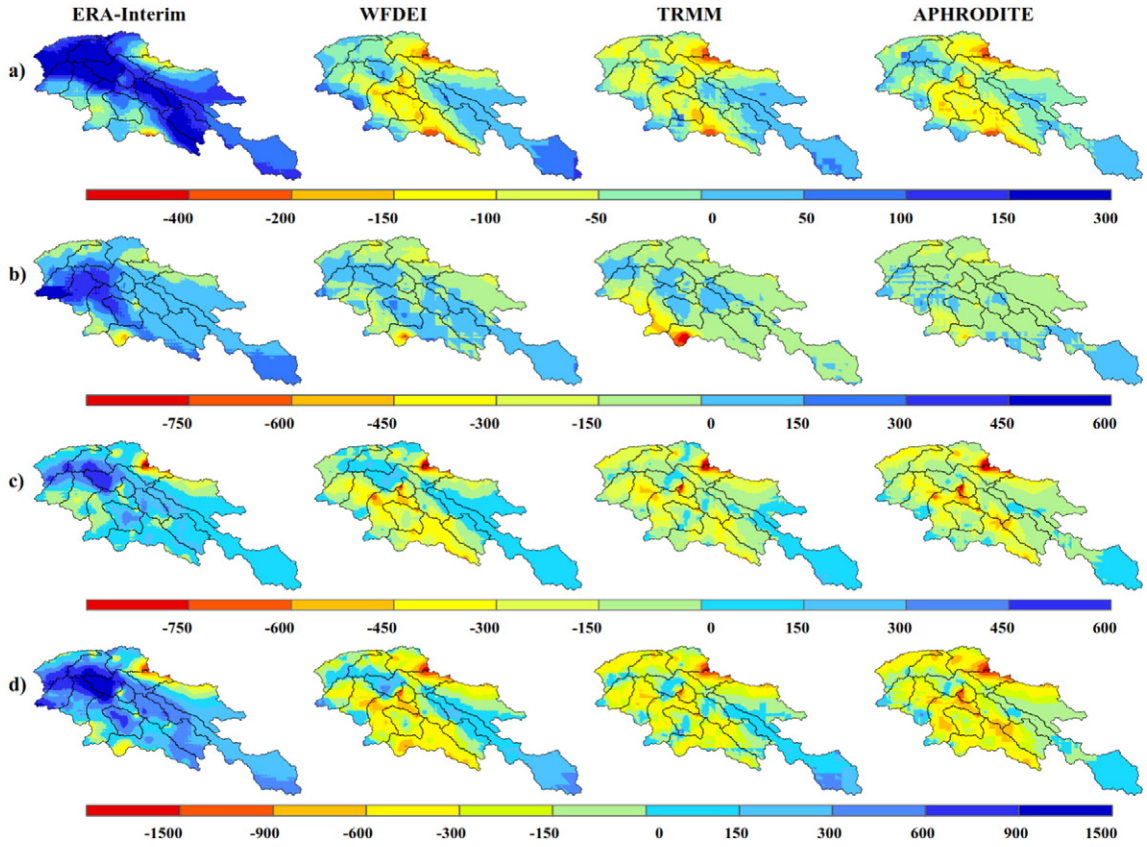

Fig. 9. Absolute bias (in mm) of ERA-Interim, WFDEI, TRMM and APHRODITE precipitation relative to the KED-based estimated precipitation for a) pre-monsoon, b) monsoon, c) winter and d) annual basis (note the different colour scales).

higher than 4000 m which is attained by 57% of the study area, are the major complexities. Generally, precipitation tends to decrease with increasing latitude (from south to north), while longitude has seasonal influence, positive in monsoon and negative in winter season. Similarly, the southeastward and southwestward orientated locations mostly receive more precipitation in monsoon and winter seasons respectively. However, the areas under the influence of rain shadow are notable exceptions, where precipitation tends to be far less throughout the year.

The core characteristics and spatial pattern of mean seasonal and annual precipitation estimates show strong south–north precipitation gradients containing the general rainfall maxima along the southern and lower most slopes of Chenab, Jhelum, Indus main and Swat basins (Fig. 5), which was also observed in previous studies (e.g. Palazzi et al., 2013; Bookhagen and Burbank, 2006). However, the unique distribution revealed by this study is the emergence of an unusually wet zone containing the 2nd precipitation maxima along the northern boundary of central Karakoram region, which had never been detected by the earlier datasets or studies. Despite the fact that this zone in the central Karakoram region accommodates some of the largest glaciers (e.g. Baltoro, Approach, Whaleback, Hispar, Biafo and Khurdopin), most of which are believed to be stable or even surging with a net positive glacier mass balance, the earlier datasets consistently and significantly underestimated precipitation in this region. However, to sustain and surge, the glaciers in this area essentially require more precipitation

Table 5
Basin-wide, seasonal and annual correction factors for each gridded precipitation product.

River basin	Pre-monsoon				Monsoon				Winter				Annual			
	ERAI	WEI	TRM	APH	ERAI	WEI	TRM	APH	ERAI	WEI	TRM	APH	ERAI	WEI	TRM	APH
Indus-U	0.21	0.37	0.52	0.86	0.36	0.57	0.63	0.96	0.47	0.35	0.59	1.05	0.32	0.45	0.59	0.95
Zanskar	0.33	0.89	1.01	1.70	0.61	0.84	0.83	1.80	0.66	1.53	1.72	2.81	0.59	1.23	1.30	2.41
Shingo	0.46	1.18	1.11	1.84	0.53	0.79	0.80	1.67	0.60	1.53	1.97	3.02	0.56	1.26	1.35	2.41
Indus-Khar	0.27	0.60	0.71	1.19	0.44	0.66	0.70	1.25	0.53	0.78	1.04	1.72	0.42	0.74	0.86	1.49
Shyok	0.49	1.22	1.35	1.73	0.84	8.74	1.45	2.32	1.08	1.03	2.38	2.61	0.82	1.53	1.75	2.41
Shigar	1.12	2.55	3.29	2.57	1.38	7.67	1.56	3.35	1.81	2.61	4.52	6.30	1.53	2.93	3.17	4.23
Hunza	0.77	2.06	2.27	2.77	1.07	9.75	1.62	3.87	1.12	1.60	2.33	5.49	1.04	2.29	2.11	4.23
Gilgit	0.42	1.16	1.58	1.22	0.74	2.11	1.46	2.72	0.48	0.88	2.23	3.23	0.52	1.17	1.79	2.22
Astore	0.65	1.85	1.82	1.75	0.57	1.26	1.17	2.37	0.84	2.08	3.22	4.11	0.74	1.86	2.07	2.82
Indus-M	0.45	1.24	1.70	1.33	0.42	1.05	0.92	1.93	0.38	0.85	1.82	2.21	0.40	0.99	1.43	1.73
Indus-L	0.77	1.09	1.32	1.11	0.51	1.03	1.01	1.11	0.92	1.51	2.01	1.80	0.71	1.27	1.47	1.37
Indus-Tar	0.47	1.09	1.30	1.50	0.64	3.43	1.07	1.94	0.76	1.08	1.84	2.60	0.63	1.24	1.43	2.09
Chitral	0.50	1.03	1.73	1.27	0.96	1.42	1.56	2.47	0.72	1.09	4.44	2.98	0.69	1.10	1.88	2.14
Swat	0.70	1.03	1.28	1.11	0.39	0.88	0.93	1.02	0.86	1.38	1.43	1.36	0.62	1.18	1.27	1.22
Jhelum	0.91	1.56	1.32	1.54	0.68	0.98	0.96	1.41	0.87	1.90	1.51	1.80	0.82	1.51	1.27	1.63
Chenab	0.84	1.70	1.47	1.83	0.80	1.05	0.76	1.35	0.87	2.58	1.75	2.11	0.89	1.77	1.28	1.84

than their ablation/discharges. Our estimates of higher precipitation coherently follow the pattern and extent of the glacier cover in the high-altitude areas. Contrary to the inconsistent and contrasting estimates by the earlier studies, this study estimated significantly higher precipitation in all the sub-basins, which are comparable and consistent with the corresponding specific runoffs (measured flows). Similarly, the drier areas under the influence of rain shadow, which are often ignored and usually overestimated by the gridded datasets, are also well recognized.

The basin-wide estimated precipitation and corresponding values of specific runoff shown in Table 3 do not support the idea of a positive mass balance in the study area. Higher values of specific runoff for Gilgit, Astore, Shyok and Shigar basins suggest essentially a negative mass balance in these basins. Similarly, Chenab, Hunza and Chitral basins show slightly higher precipitation and may have neutral to slightly negative mass balance. Swat, Jhelum and Chenab basins indicate precipitation greater than river flows. However, evapotranspiration and percolation losses from these basins may be relatively large due to higher temperatures (large area below the 0 °C isotherm), greater vegetative cover and availability of moisture for evapotranspiration/percolation (more runoff from rainfall and seasonal snow). Thus, these basins may also be considered to have neutral to negative mass balance. The estimates for Zanskar basin and Ladakh region in the TP are relatively uncertain due to very low number of observation points in these areas. The precipitation estimates relative to the corresponding river flow for the Indus at Kharmong basin seem to be on the high side. Therefore, a neutral to negative mass balance can be expected for this catchment. The Indus at Tarbela combines drainage of the upstream catchments, which are either neutral or experience a negative mass balance. However, the net impact is likely to be a negative mass balance as precipitation is only marginally higher than the specific runoff. Our results are in good agreement to available glacier mass balance studies (e.g. Gardelle et al., 2012; Kaab et al., 2012, 2015).

The selected gridded precipitation products provide only a marginal resemblance of the actual precipitation. ERA-Interim largely overestimates precipitation in all the sub-basins except Shigar and Hunza, while the other three datasets consistently underestimate precipitation in all the areas barring Ladakh region of the TP (Indus-U up to Kharmong). The overestimated precipitation in the TP region by the APHRODITE and TRMM 3B43 products was also observed by Palazzi et al. (2013), Prakash et al. (2013), Andermann et al. (2011) and Yin et al. (2008). ERA-Interim is prone to underestimate precipitation by up to 40% in the areas with low evaporation rates and overestimate by about 150% under conditions with high evaporation rates (Bumke, 2015). The overall underestimated precipitation by WFDEI and TRMM datasets, also observed by Li et al. (2013), may be attributed to the fact that their correction/validation is done mainly by the use of stations predominantly located in valley bottoms. This was also reported by Reggiani and Rientjes (2015) who observed un-corrected reanalysis data from ERA-Interim and NCEP/NCAR products as the better option in terms of quantitative estimates of precipitation in the UIB up to Besham Qila. Several studies (e.g. Andermann et al., 2011; Rajeevan and Bhate, 2009; Krishnamurti et al., 2009; Yatagai and Kawamoto, 2008; Yatagai and Xie, 2006) consider APHRODITE as an accurate dataset, but its accuracy greatly depends on the density of station data in the area of interest. In the high-altitude areas of the Indus basin, the APHRODITE product uses non-representative low-altitude stations to derive the spatial distribution of high-altitude precipitation. Therefore, it reflects highly underestimated precipitation in all of the sub-basins. Moreover, the four gridded products completely fail to reproduce the zone of 2nd precipitation maxima in the central Karakoram and could not properly detect the drier areas under the influence of rain shadow. They tend to smooth the precipitation due to their lower spatial resolution resulting in significant overestimated precipitation in these areas. This study incorporates high-altitude observations, which have never been used in the formation or validation of precipitation datasets. The KED-based interpolation scheme further amplifies the precipitation at the higher altitudes by taking into account the spatial autocorrelation and elevation effects at local scale. The pattern statistics indicate that despite better quantitative estimates, ERA-Interim and WFDEI products are relatively poor in reproducing the spatial pattern of estimated precipitation mainly due to their lower spatial resolution and use of non-representative data in their formation and/or validation. The relatively better patterns shown by APHRODITE are due to the fact that this dataset is derived from station observations.

In view of significant biases in the gridded precipitation products covering this region, we determined basin-wide seasonal and annual correction factors for each dataset. These correction factors can be used for lumped hydrological modelling studies. Like, Lutz et al. (2014a) appropriately multiplied APHRODITE precipitation by a constant factor of 1.17 to account for the inherent underestimation and avoid undue compensation by suboptimal input parameters. However, this factor is still on the lower end as our analysis suggests an average correction factor of 2.1 for the UIB up to Tarbela dam, which varies significantly for all other sub-basins. Hence, the use of underestimated precipitation by Lutz et al. (2014a) might have resulted in an exaggerated snow/glacier melt contribution and a biased conclusion of the associated snow/glacier cover extent. Nevertheless, our KED-based precipitation estimates and correction factors can efficiently be used for bias correction of any gridded precipitation product and improved hydro-climate assessments for the study area.

Although, the methods employed in this study are straightforward and robust, further improvements in precipitation estimation can be expected once higher quality observed data with more spatiotemporal coverage, particularly above 4000 m a.s.l., become available. Moreover, the employed methods are equally applicable for other regions of the world, especially with similar geo-hydro-climatological conditions.

6. Conclusions

Precipitation in the high altitude areas of the Indus basin governs the renewable water resources and associated developments, but a comprehensive assessment of precipitation distribution in this region is largely lacking. Here, we attempt to explain how precipitation amounts, seasonality and patterns are represented in the study area. The altitudinal analysis of precipitation observations in each sub-basin demonstrated the important role of orographic precipitation. Yet, the topographical variability even at the sub-basin and local scale is so high that the available observations are insufficient to infer an accurate distribution of altitudinal precipitation. Instead, rather complex and nonlinear trends of precipitation increase with altitude are evidently depicted.

The study provides much improved estimates of precipitation distribution, which are comparable and consistent with the corresponding observed runoffs from the 12 sub-basins. The geo-statistical analysis of precipitation observations revealed substantially higher precipitation in most of the sub-basins compared to earlier studies. The study area largely experiences a bimodal weather system reflecting wintertime precipitation associated with the westerly systems and the impact of Indian summer monsoon. The analysis demonstrated two distinct rainfall maxima; 1st along southern and lower most slopes of Chenab, Jhelum, Indus main and Swat basins, and 2nd around north-west corner of Shyok basin in the central Karakoram. Moreover, the estimates better recognize the drier areas under the influence of rain shadow, which are often overlooked by the gridded datasets.

Our analysis shows that the selected gridded precipitation products derived from four different sources are prone to significant errors providing only a marginal resemblance of the actual precipitation in the study area. We conclude that the uncorrected gridded precipitation products are highly unsuitable to estimate precipitation distribution and to derive glacio-hydrological models in water balance studies in the high-altitude areas of Indus basin. The suggested basin-wide

seasonal and annual correction factors for the four gridded precipitation products can be useful for lumped hydrological modelling studies. The estimated precipitation distribution can effectively serve as a basis for bias correction of any gridded precipitation products for the study area.

Acknowledgements

This research work is supported by the Dutch Ministry of Foreign Affairs through the Netherlands Fellowship Program (NFP-PhD.11/898) under the budget for development cooperation and partially carried out under the Himalayan Adaptation Water and Resilience (HI-AWARE) consortium supported by the Collaborative Adaptation Research Initiative in Africa and Asia (CARIAA) with funding from the UK Government's Department for International Development and the International Development Research Centre, Ottawa, Canada. The views expressed in this work do not necessarily represent those of the supporting organizations. The authors express their deepest gratitude to WAPDA and PMD for sharing the hydro-meteorological data of the study region, especially to all the anonymous observers who have collected the data. Ev-K2-CNR and GHCN are also appreciated for ensuring online availability of their climatic data. The authors also acknowledge the institutions and the teams responsible for the creation and distribution of the ERA-Interim, WFDEI, TRMM and APHRODITE precipitation products. Useful input offered by the anonymous reviewers is also duly acknowledged.

Appendix A

Details of meteorological stations used in this study. The stations mentioned at S. No. 1–21 are operated by PMD, 22–65 by WAPDA, 66–67 by Ev-K2-CNR, 68–108 by IMD (taken from GHCN), 109–118 by University of Boon's CAK project (synthesized from Winiger et al., 2005; Miehe et al., 1996, 2001; Eberhardt et al., 2007), and 119–134 are virtual stations detailed at Table 1.

Sr. no.	Station name	Lat (dd)	Long (dd)	Elevation (m)	Data period	Sr. no.	Station name	Lat (dd)	Long\(dd)	Elevation (m)	Data period
1	Astore	35.3667	74.9000	2394	1954–2012	68	Bhadarwah	32.9667	75.7167	1690	1911–1968
2	Babusar	35.1458	74.0444	4160	2005–2012	69	Banihal	33.5000	75.1700	1630	1961–1970
3	Balakot	34.5500	72.3500	995	1957–2012	70	Baramula	34.2000	74.3700	1572	1902–1970
4	Bunji	35.6667	74.6333	1372	1953–2012	71	Charisharif	33.8700	74.7700	1616	1960–1970
5	Chilas	35.4167	74.1000	1251	1953–2013	72	Digar	34.2500	77.7500	5182	1956–1964
6	Chitral	35.8500	71.8333	1498	1964–2012	73	Dras	34.4333	75.7667	3066	1901–1968
7	Dir	35.2000	71.8500	1425	1967–2010	74	Durroo	33.5700	75.2300	1790	1924–1964
8	Drosh	35.5667	71.7833	1464	1951–2012	75	Gondla	32.5200	77.0300	3144	1951–1970
9	GD Poto	34.2167	73.6167	814	1955–2012	76	Gulmarg	34.0500	74.4000	2655	1951–1971
10	Gilgit	35.9167	74.3333	1460	1951–2012	77	Gund	34.2500	75.0800	2052	1956–1970
11	Gupis	36.1667	73.4000	2156	1955–2012	78	Gurez	34.6300	74.8500	2417	1933–1958
12	Hunza	36.3220	74.6460	2374	2007–2012	79	Handwara	34.4000	74.2800	1585	1958–1970
13	Kakul	34.1833	73.2500	1308	1952–2012	80	Inshan	33.7500	75.5000	2440	1971–1980
14	Kotli	33.5167	73.9000	614	1953–2012	81	Kargil	34.5700	76.1300	2679	1908–1966
15	Malakand	34.5500	71.9167	800	2003–2008	82	Khaltse	34.2500	76.8333	3205	1956–1970
16	Malamjaba	34.7500	72.9000	2591	2003–2008	83	Khangral	34.3333	76.5000	3887	1956–1971
17	Murree	33.9000	73.4000	2168	1980–2012	84	Kishtwar	33.3000	75.7500	1215	1901–1970
18	Muzaffarabad	34.3667	73.4833	702	1955–2012	85	Kokernagh	33.9200	75.2800	1676	1960–1970
19	Pattan	35.1000	73.0000	752	2004–2012	86	Koksar	32.4160	77.2190	3507	1951–1970
20	Saidusharif	34.7333	72.3500	961	1974–2010	87	Kukernag	33.6000	75.3000	1865	1961–1970
21	Skardu	35.3000	75.6833	2210	1952–2012	88	Kulgam	33.6300	75.0200	1615	1902–1970
22	Besham	34.9333	72.8833	480	1971–2003	89	Kyelong	32.5833	77.0667	3500	1903–1970
23	Burzil	34.9056	75.0917	4030	1999–2012	90	Langet	34.3700	74.3000	1588	1916–1970
24	Dagar	34.5100	72.4864	732	1984–2001	91	Leh	34.1500	77.5667	3514	1876–1969
25	Deosai	35.1000	75.6000	3910	1995–2011	92	Matsal	33.9833	76.6167	4325	1971–1981
26	Dhudnial	34.7000	74.1170	534	1984–1997	93	Mulbek	34.3333	76.3333	3926	1956–1969
27	Domel	34.3678	73.4689	686	1984–2001	94	Nowshera	33.1500	74.2300	599	1913–1969
28	Doyian	35.5450	74.7042	2454	1979–2003	95	Panamik	34.7500	77.5000	4056	1956–1970
29	Gujar Khan	33.2500	73.3000	457	1984–2001	96	Pendras	34.4167	75.5833	4880	1956–1971
30	Hushy	35.3667	76.4000	3010	1994–2010	97	Phalgam	34.0300	75.3300	1707	1960–1972
31	Jabbar	34.6717	73.2278	2134	1984–2001	98	Prang	34.2800	74.8700	1588	1960–1973
32	Kalam	35.4700	72.6010	2744	1984–2010	99	Qazi Gund	33.5800	75.0800	1690	1962–1974
33	Kallar	33.4167	73.3667	518	1984–2001	100	Ramban	33.2500	75.2500	945	1901–1969
34	Kelash	35.6955	71.6547	2810	2000–2013	101	Riasi	33.0800	74.8300	585	1901–1970
35	Khandar	33.5000	74.0500	1067	1984–2001	102	Shiquanhe	32.5000	80.0830	4280	1962–2012
36	Khot	36.5167	72.5833	3505	1994–2012	103	Shopian	33.7200	74.8300	1615	1960–1970
37	Khunjrab	36.8500	75.4000	4730	1995–2012	104	Sonemarg	34.3167	75.3167	2515	1902–1969
38	Kotli	33.4847	73.8811	610	1984–2001	105	Sopore	34.3000	74.4700	1574	1930–1970
39	Lora	33.8833	73.2833	1482	1989–1992	106	Srinagar	34.0833	74.8333	1587	1993–2013
40	Mangla	33.1333	73.6333	305	1984–2001	107	Uttamchipura	34.5000	74.6700	3145	1901–1956
41	Naltar	36.2167	74.2667	2810	1995–2012	108	Verinagh	33.5300	75.2500	1646	1965–1970
42	Naran	34.9000	73.6500	2363	1984–2001	109	Alambar	36.7000	73.4833	4400	1991–1999
43	Oghi	34.5000	73.0167	1128	1984–2001	110	Bagrot	36.0167	74.5500	2310	1993–2009
44	Palandri	33.7167	73.7000	1402	1984–2001	111	Bulibalsirbar	36.3667	73.2500	4050	1991–1999
45	Phulra	34.3333	73.0833	915	1984–2001	112	Garmashbar	36.5167	73.5333	3600	1991–1999
46	Pir Chenasi	34.3850	73.5450	2650	2004–2013	113	Khaimetbar	36.5000	73.0500	3600	1991–1999
47	Puran	34.7500	72.7000	1067	1984–2001	114	Khunjrab	36.8800	74.4167	4700	1993–2012
48	Rama	35.3583	74.8056	3140	1999–2012	115	Dadormal	36.0167	74.4167	3780	1991–1999
49	Ratu	35.1528	74.8056	2920	1999–2013	116	Dame	36.0500	74.6667	3560	1991–1999
50	Rawlakot	33.8667	74.2667	1677	1984–2001	117	Diran	36.0500	74.6000	3650	1991–1999

(continued on next page)

(*continued*)

Sr. no.	Station name	Lat (dd)	Long (dd)	Elevation (m)	Data period	Sr. no.	Station name	Lat (dd)	Long\(dd)	Elevation (m)	Data period
51	Saifulmulk	34.8438	73.6875	3200	2000–2013	118	Baldihel	36.3500	74.8000	3900	1994–1996
52	Sehrkakota	33.7333	73.9667	915	1984–2001	119	Sentik	33.9967	75.9500	4908	1963–1980
53	Shahpur	34.9167	72.6667	2012	1984–2001	120	Nun Kun N	34.1219	76.1014	5200	1973–1980
54	Shangla	34.8808	72.5908	2160	2000–2007	121	Batura	36.6667	74.3833	4840	1973–1974
55	Shendure	36.0861	72.5250	3719	1994–2012	122	Baltoro	35.8778	76.5508	5500	1973–1980
56	Shigar	35.5300	75.5917	2470	1996–2012	123	Urdok	35.7669	76.7025	5400	2004–2006
57	Shinkiari	34.4667	73.2667	991	1984–2001	124	Whaleback	36.0572	75.5915	4900	1985–1986
58	Shogran	34.6200	73.4856	3205	2000–2013	125	Approach	36.0678	75.6331	5100	1985–1987
59	Tandar	33.2039	73.9764	671	1984–2001	126	Hispar East	35.8495	75.5064	4830	1985–1988
60	Tarbela	34.0667	72.7700	610	1984–2001	127	Hispar Pass	36.0281	75.5215	5100	1984–1986
61	Ushkore	36.0175	73.3583	3353	1999–2012	128	Hispar Dome	36.0109	75.5187	5450	1982–1986
62	Yasin	36.6333	73.3000	3353	1999–2013	129	Khurdopin	36.1338	75.6197	5520	1984–1986
63	Yugo	35.1833	76.1000	2469	1984–2001	130	Nanga Parbat	35.1672	74.4444	4500	1984–1997
64	Zani	36.2833	72.1500	3000	1994–2012	131	Siachin A	35.4707	77.0376	4800	1986–1991
65	Ziarat	36.8333	74.2778	3669	1995–2012	132	Siachin B	35.5235	76.9915	4950	1986–1992
66	Askole	35.6806	75.8153	3015	2005–2008	133	Siachin C	35.5187	76.9116	5050	1986–1993
67	Urdukas	35.7281	76.2861	3926	2004–2008	134	Siachin D	35.6242	76.8592	5350	1986–1994

References

Ahmad, S., Nishii, K., Tamura, T., Ohta, T., Ikoma, E., Kitsuregawa, M., Koike, T., 2012. Characteristics of climatological tropospheric conditions during pre-monsoon and matured phases of Pakistan summer monsoon. Annu. J. Hydraul. Eng. JSCE 56, 1–6.

Akhtar, M., Ahmad, N., Booij, M.J., 2008. The impact of climate changes on the water resources of Hindukush–Karakorum–Himalaya region under different glacier coverage scenarios. J. Hydrol. 355, 148–163. http://dx.doi.org/10.1016/j.jhydrol.2008.03.015.

Alpert, P., 1986. Mesoscale indexing of the distribution of orographic precipitation over high mountains. J. Clim. Appl. Meteorol. 25 (4), 532–545. http://dx.doi.org/10.1175/1520-0450(1986)025<0532:MIOTDO>2.0.CO;2.

Andermann, C., Bonnet, S., Gloaguen, R., 2011. Evaluation of precipitation datasets along the Himalayan front. Geochem. Geophys. Geosyst. 12 (7). http://dx.doi.org/10.1029/2011GC003513.

Archer, D.R. (2001), The Climate and Hydrology of Northern Pakistan With Respect to the Assessment of Flood Risk to Hydropower Schemes. Unpublished Report, GTZ/WAPDA, Lahore.

Archer, D.R., Fowler, H.J., 2004. Spatial and temporal variations in precipitation in the Upper Indus Basin, global teleconnections and hydrological implications. Hydrol. Earth Syst. Sci. 8 (1), 47–61. http://dx.doi.org/10.5194/hess-8-47-2004.

Arora, M., Singh, P., Goel, N.K., Singh, R.D., 2006. Spatial distribution and seasonal variability of rainfall in a mountainous basin in the Himalayan region. Water Resour. Manag. 20, 489–508. http://dx.doi.org/10.1007/s11269-006-8773-4.

Bajracharya, S.R., Shrestha, B. (Eds.), 2011. The Status of Glaciers in the Hindu Kush–Himalayan region. ICIMOD, Kathmandu (http://lib.icimod.org/record/9419).

Berrisford, P., Dee, D., Poli, P., Brugge, R., Fielding, K., Fuentes, M., Kallberg, P., Kobayashi, S., Uppala, S., Simmons, A., 2011. The ERA-Interim Archive, Version 2.0, European Centre for Medium Range Weather Forecasts Shinfield Park, Reading, Berkshire RG2 9AX, United Kingdom.

Bhambri, R., Bolch, T., Kawishwar, P., Dobhal, D.P., Srivastava, D., Pratap, B., 2013. Heterogeneity in glacier response in the upper Shyok valley, northeast Karakoram. Cryosphere 7, 1385–1398. http://dx.doi.org/10.5194/tc-7-1385-2013.

Bhutiyani, M.R., 1999. Mass balance studies on Siachen glacier in the Nubra valley, Karakoram Himalaya, India. J. Glaciol. 45 (149), 112–118.

BIG, 1979. The Batura Glacier in the Karakoram Mountains and its variations, Batura Investigations Group. Sci. Sinica 22, 958–974.

Bishop, T.F.A., McBratney, A.B., 2001. A comparison of prediction methods for the creation of field-extent soil property maps. Geoderma 103, 149–160.

Bocchiola, D., Diolaiuti, G.A., Soncini, A., Mihalcea, C., D'Agata, C., Mayer, C., Lambrecht, A., Rosso, R., Smiraglia, C., 2011. Prediction of future hydrological regimes in poorly gauged high altitude basins: the case study of the upper Indus, Pakistan. Hydrol. Earth Syst. Sci. 15, 2059–2075 s.

Bolch, T., Kulkarni, A., Kääb, A., Hugget, C., Paul, F., Cogley, J.G., Frey, H., Kargel, J.S., Fujita, K., Scheel, M., Bajracharya, S., Stoffel, M., 2012. The state and fate of Himalayan glaciers. Science 336, 310–314.

Bookhagen, B., Burbank, D.W., 2006. Topography, relief, and TRMM-derived rainfall variations along the Himalaya. Geophys. Res. Lett. 33 (8), L08405. http://dx.doi.org/10.1029/2006GL026037.

Bookhagen, B., Burbank, D.W., 2010. Toward a complete Himalayan hydrological budget: spatiotemporal distribution of snowmelt and rainfall and their impact on river discharge. J. Geophys. Res. Earth Surf. 115 (3), 2003–2012.

Bourennane, H., King, D., Couturier, A., 2000. Comparison of kriging with external drift and simple linear regression for predicting soil horizon thickness with different sample densities. Geoderma 97, 255–271.

Bumke, K., 2015. (2015), Validation of ERA-Interim precipitation estimates over the Baltic Sea. Geophys. Res. Abstr. 17, EGU2015–EGU3035.

Burrough, P.A., McDonnell, R.A., 1998. Principles of Geographical Information Systems. Oxford University Press, Oxford 333 pp.

Cogley, J.G., 2011. Present and future states of Himalaya and Karakoram glaciers. Ann. Glaciol. 52 (59), 69–73.

CWC, NRSC, 2014. Indus Basin, Version 2.0, Central Water Commission and National Remote Sensing Centre. Government of India, Ministry of Water Resources.

Decheng, M., 1978. The Map of Snow Mountains in China, K2 (Mount Quogori), Lanzhou, Chinese Academy of Sciences. Lanzhou Institute of Glaciology and Geocryology.

Dee, D.P., Uppala, S.M., Simmons, A.J., Berrisford, P., Poli, P., Kobayashi, S., Andrae, U., Balmaseda, M.A., Balsamo, G., Bauer, P., Bechtold, P., Beljaars, A.C.M., van de Berg, L., Bidlot, J., Bormann, N., Delsol, C., Dragani, R., Fuentes, M.,., Geer, A.J., Haimberger, L., Healy, S.B., Hersbach, H., Hólm, E.V., Isaksen, L., Kå llberg, P.,., Köhler, M., Matricardi, M., McNally, A.P., Monge-Sanz, B.M., Morcrette, J.-J., Park, B.-K., Peubey, C., de Rosnay, P., Tavolato, C., Thépaut, J.-N., Vitart, F., 2011. The ERA-Interim reanalysis: configuration and performance of the data assimilation system. Q. J. R. Meteorol. Soc. 137, 553–597. http://dx.doi.org/10.1002/qj.828,2011.4757,4759,4775.

Dhar, O.N., Rakhecha, P.R., 1981. In: Lighthill, J., Pearce, R.P. (Eds.), The Effect of Elevation on Monsoon Rainfall Distribution in the Central Himalayas, in Monsoon Dynamics. Cambridge University Press, New York, pp. 253–260 http://dx.doi.org/10.1017/CBO9780511897580.020.

Diggle, P.J., Ribeiro, P.J., 2007. Model-based Geostatistics. Springer Series in Statistics.

Ding, Y.H., Chan, J.C.L., 2005. The East Asian summer monsoon: an overview. Meteorog. Atmos. Phys. 89, 117–142.

Eberhardt, E., Dickore, W.B., Miehe, G., 2007. Vegetation Map of the Batura Valley (North Pakistan). Erdkundi. 61, pp. 93–112.

Filippi, L., Palazzi, E., von Hardenberg, J., Provenzale, A., 2014. Multidecadal variations in the relationship between the NAO and winter precipitation in the Hindu-Kush Karakoram. J Clim. http://dx.doi.org/10.1175/JCLI-D-14-00286.1.

Fowler, H.J., Archer, D.R., 2006. Conflicting signals of climate change in the Upper Indus basin. J. Clim. 19, 4276–4293.

Gardelle, J., Berthier, E., Arnaud, Y., 2012. Slight mass gain of Karakoram glaciers in the early 21st century. Nat. Geosci. 5, 322–325. http://dx.doi.org/10.1038/NGEO1450.

Gardelle, J., Berthier, E., Arnaud, Y., Kääb, A., 2013. Region-wide glacier mass balances over the Pamir–Karakoram–Himalaya during 1999–2011. Cryosphere 7, 1263–1286. http://dx.doi.org/10.5194/tc-7-1263-2013.

Gardner, A.S., Moholdt, G., Cogley, J.G., B., W.,s., Arendt, A.A., Wahr, J., Berthier, E.,., Hock, R., Pfeffer, W.T., Kaser, G., Ligtenberg, S.R.M., Bolch, T., Sharp, M.J., Hagen, J.O., van den Broeke, M., Paul, F., 2013. A reconciled estimate of glacier contributions to sea level rise: 2003 to 2009. Science 340, 852–857. http://dx.doi.org/10.1126/science.1226558 (2013).

Goovaerts, P., 2000. Geostatistical approaches for incorporating elevation into the spatial interpolation of rainfall spatial interpolation of rainfall. J. Hydrol. 228, 113–129.

Haberlandt, U., 2007. Geostatistical interpolation of hourly precipitation from rain gauges and radar for a large-scale extreme rainfall event. J. Hydrol. 332, 144–157.

Harris, I., Jones, P.D., Osborn, T.J., Lister, D.H., 2013. Updated high-resolution grids of monthly climatic observations—the CRU TS3.10 dataset. Int. J. Climatol. 34, 623–642. http://dx.doi.org/10.1002/joc.3711.

Hartkamp, A.D., DeBeurs, K., Stein, A., White, J.W., 1999. Interpolation Techniques for Climate Variables, Geographic Information Systems. vol. 99-01. CIMMYT Natural Resources Group, Mexico.

Hasson, S., Lucarini, V., Khan, M.R., Petitta, M., Bolch, T., Gioli, G., 2014. Early 21st century snow cover state over the western river basins of the Indus River system. Hydrol. Earth Syst. Sci. 18, 4077–4100. http://dx.doi.org/10.5194/hess-18-4077-4100.

Hengl, T., Geuvelink, G.B.M., Stein, A., 2003. Comparison of Kriging With External Drift and Regression Kriging. Technical Note, ITC (https://www.itc.nl/library/Papers_2003/misca/hengl_comparison.pdf).

Hewitt, K., 2005. The Karakoram anomaly? Glacier expansion and the 'elevation effect', Karakoram Himalaya. Mt. Res. Dev. 25, 332–340. http://dx.doi.org/10.1659/0276-4741(2005)025[0332:TKAGEA]2.0.CO;2.

Hewitt, K., 2006. Glaciers of the Hunza basin and related features. In: Kreutzmann, H. (Ed.), Karakoram in Transition: Culture, Development and Ecology in the Hunza Valley. Oxford University Press, Oxford, United Kingdom, pp. 49–72.

Hewitt, K., 2011. Glacier change, concentration, and elevation effects in the Karakoram Himalaya, Upper Indus Basin. Mt. Res. Dev. 31 (3), 188–200. http://dx.doi.org/10.1659/mrd-journal-d-11-00020.1.

Hewitt, K., 2013. Glaciers of the Karakoram Himalaya: Glacial Environments, Processes, Hazards and Resources. Springer Dordrecht Heidelberg New York London http://dx.doi.org/10.1007/978-94-007-6311-1.
NOAA-NCDC, Monthly Summaries of the Global Historical Climatology Network - Daily (GHCN-D), NOAA National Climatic Data Center, http://www.ncdc.noaa.gov/cdo-web/datasets (accessed in June, 2014).
Huffman, G.J., Adler, R.F., Bolvin, D.T., Gu, G., Nelkin, E.J., Bowman, K.P., Hong, Y., Stocker, E.F., Wolff, D.B., 2007. The TRMM Multisatellite Precipitation Analysis (TMPA): quasiglobal, multiyear, combined-sensor precipitation estimates at fine scales. J. Hydrometeorol. 8, 38–55. http://dx.doi.org/10.1175/JHM560.1.
ICES, 2005. Report of the Working Group on Marine Habitat Mapping (WGMHM), ICES CM 2005/E:05. Bremerhaven, Germany.
Immerzeel, W.W., Droogers, P., de Jong, S.M., Bierkens, M.F.P., 2009. Large-scale monitoring of snow cover and runoff simulation in Himalayan river basins using remote sensing. Remote Sens. Environ. 113, 40–49.
Immerzeel, W.W., Droogers, P., de Jong, S.M., Bierkens, M.F.P., 2010. Satellite Derived Snow and Runoff Dynamics in the Upper Indus River Basin, Grazer Schriften der Geographie und Raumforschung Band 45/2010 pp.303–312.
Immerzeel, W.W., Pellicciotti, F., Shrestha, A.B., 2012. Glaciers as a proxy to quantify the spatial distribution of precipitation in the Hunza basin. Mt. Res. Dev. 32 (1), 30–38. http://dx.doi.org/10.1659/MRD-JOURNAL-D-11-00097.1.
Immerzeel, W.W., Petersen, L., Ragettli, S., Pellicciotti, F., 2014. The importance of observed gradients of air temperature and precipitation for modeling runoff from a glacierised watershed in the Nepalese Himalayas. Water Resour. Res. 50, 2212–2226. http://dx.doi.org/10.1002/2013WR014506.
Immerzeel, W.W., Wanders, N., Lutz, A.F., Shea, J.M., Bierkens, M.F.P., 2015. Reconciling high altitude precipitation in the upper Indus Basin with glacier mass balances and runoff. Hydrol. Earth Syst. Sci. 19 (4673–4687), 2015. http://dx.doi.org/10.5194/hessd-12-4755-2015.
Jacob, T., Wahr, J., Pfeffer, W.T., Swenson, S., 2012. Recent contributions of glaciers and ice caps to sea level rise. Nature 482, 514–518.
Kaab, A., Berthier, E.N., Christopher, Gardelle, J., Arnaud, Y., 2012. Contrasting patterns of early twenty-first-century glacier mass change in the Himalayas. Nature 488 (7412), 495–498 (doi: http://www.nature.com/nature/journal/v488/n7412/abs/nature11324.html#supplementary-information).
Kaab, A., Treichler, D., Nuth, C., Berthier, E., 2015. Brief Communication: contending estimates of 2003–2008 glacier mass balance over the Pamir–Karakoram–Himalaya. Cryosphere 9 (557–564), 2015. http://dx.doi.org/10.5194/tc-9-557-2015.
Karki, M.B., Shrestha, A.B., Winiger, M., 2011. Enhancing knowledge management and adaptation capacity for integrated management of water resources in the Indus River Basin. Mt. Res. Dev. 31 (3), 242–251. http://dx.doi.org/10.1659/MRD-JOURNAL-D-11-00017.1 2011.
Khan, A., Richards, K.S., Parker, G.T., McRobie, A., Mukhopadhyay, B., 2014. How large is the Upper Indus Basin? The pitfalls of auto-delineation using DEMs. J. Hydrol. 509 (0), 442–453. http://dx.doi.org/10.1016/j.jhydrol.2013.11.028.
Kick, W., 1980. Material for a glacier inventory of the Indus drainage basin—the Nanga Parbat massif, World Glacier Inventory. (Proceedings of the Riederalp Workshop, September 1978: IAHS-AISH Publ. no. 126, p. 1980.
Krishnamurti, T.N., Kishtawal, C.M., 2000. A pronounced continental-scale diurnal mode of the Asian summer monsoon. Mon. Weather Rev. AMS 128, 462–473.
Krishnamurti, T.N., Mishra, A.K., Simon, A., Yatagai, A., 2009. Use of a dense gauge network over India for improving blended TRMM products and downscaled weather models. J. Meteorol. Soc. Jpn. 87, 395–416.
Li, J., Heap, A.D., 2011. A review of comparative studies of spatial interpolation methods in environmental sciences: performance and impact factors. Ecol. Inform. 6 (3–4), 228–241. http://dx.doi.org/10.1016/j.ecoinf.2010.12.003.
Li, J., Heap, A.D., 2014. Spatial interpolation methods applied in the environmental sciences: a review. Environ. Model Softw. 53 (2014), 173–189http://dx.doi.org/10.1016/j.envsoft.2013.12.008.
Li, C., Yanali, M., 1996. The onset and interannual variability of the Asian summer monsoon in relation to land–sea thermal contrast. J. Clim. 9, 358–375. http://dx.doi.org/10.1175/1520-0442(1996)009<0358:TOAIVO>2.0.CO;2.
Li, L., Xu, C.-Y., Zhang, Z., Jain, S.K., 2013. Validation of a new meteorological forcing data in analysis of spatial and temporal variability of precipitation in India. Stoch. Env. Res. Risk A. http://dx.doi.org/10.1007/s00477-013-0745-7.
Lin, Z., Wu, X., 1990. A preliminary analysis about the tracks of moisture transport on the Qinghai–Xizang Plateau. Geogr. Res. 9, 33–40 1990 (in Chinese).
Liu, G., 1989. Hydrometeorological characteristics of the Tibet Plateau, IAHS Publ. No. 179, Atmospheric Deposition. (Proceedings of the Baltimore Symposium, pp. 267–280.
Loukas, A., Quick, M.C., 1996. Spatial and temporal distribution of storm precipitation in southwestern British Columbia. J. Hydrol. 174, 37–56.
Lutz, A.F., Immerzeel, W.W., Shrestha, A.B., Bierkens, M.F.P., 2014a. Consistent increase in high Asia's runoff due to increasing glacier melt and precipitation. Nat. Clim. Chang. http://dx.doi.org/10.1038/nclimate2237 advance online publication.
Lutz, A.F., Immerzeel, W.W., Kraaijenbrink, P.D.A., 2014b. Gridded Meteorological Datasets and Hydrological Modelling in the Upper Indus Basin, Final Report, for International Centre for Integrated Mountain Development (ICIMOD), FutureWater, Costerweg 1V, 6702 AA Wageningen, The Netherlands.
Masson, D., Frei, C., 2014. Spatial analysis of precipitation in a high-mountain region: exploring methods with multi-scale topographic predictors and circulation types. Hydrol. Earth Syst. Sci. 18, 4543–4563 (www.hydrol-earth-syst-sci.net/18/4543/2014/doi:10.5194/hess-18-4543-2014).
Mathison, C., Wiltshire, A., Dimri, A.P., Falloon, P., Jacob, D., Kumar, P., Moors, E., Ridley, J., Siderius, C., Stoffel, M., Yasunari, T., 2013. Regional projections of North Indian climate for adaptation studies. Sci. Total Environ. 468, S4–S17.
Matsuura, K., Willmott, C.J., 2009. Terrestrial precipitation: 1900–2008 gridded monthly time series, at. (accessed in July 2014) http://climate.geog.udel.edu/~climate/html_pages/download.html.
Mayer, C., Lambrecht, A., Belò, M., Smiraglia, C., Diolaiuti, G., 2006. Glaciological characteristics of the ablation zone of Baltoro glacier, Karakoram, Pakistan. Ann. Glaciol. 43 (1), 123–131. http://dx.doi.org/10.3189/172756406781812087.
Mayer, C., Lambrecht, A., Oerter, H., Schwikowski, M., Vuillermoz, E., Frank, N., Diolaiuti, G., 2014. Accumulation studies at a high elevation glacier site in central Karakoram. Adv. Meteorol., Article ID 215162 http://dx.doi.org/10.1155/2014/215162 Volume 2014.
Mayewski, P.A., Lyons, W.B., Ahmad, N., 1983. Chemical Composition of a High Altitude Fresh Snowfall in the Ladakh Himalayas. Earth Science Faculty Scholarship Paper 187. http://digitalcommons.library.umaine.edu/ers_facpub/187, (accessed in July 2014).
Mayewski, P.A., Lyons, W.B., Ahmad, N., Smith, G., Pourchet, M., 1984. Interpretation of the chemical and physical time series retrieved from Sentik glacier, Ladakh Himalaya, India. J. Glaciol. 30 (104), 66–76.
Miehe, S., Cramer, T., Jacobsen, J.-P., Winiger, M., 1996. Humidity conditions in the western Karakoram as indicated by climatic data and corresponding distribution patterns of the montane and alpine vegetation. Erdkundi. 50, pp. 190–204.
Miehe, S., Winiger, M., Bohner, J., Yili, Z., 2001. The climate diagram map of high Asia. Erdkundi. 55, pp. 94–97.
Minasny, B., McBratney, A.B., 2007. Spatial prediction of soil properties using EBLUP with the Matern covariance function. Geoderma 140, 324–336.
Minora, U., Bocchiola, D., D'Agata, C., Maragno, D., Mayer, C., Lambrecht, A., Mosconi, B., Vuillermoz, E., Senese, A., Compostella, C., Simiraglia, C., Diolaiuti, G., 2013. 2001–2010 glacier changes in the Central Karakoram National Park: a contribution to evaluate the magnitude and rate of the "Karakoram anomaly". Cryosphere Discuss. 7 (3), 2891–2941. http://dx.doi.org/10.5194/tcd-7-2891-2013.
Mukhopadhyay, B., 2012. Detection of dual effects of degradation of perennial snow and ice covers on the hydrologic regime of a Himalayan river basin by stream water availability modeling. J. Hydrol. 412–413 (0), 14–33. http://dx.doi.org/10.1016/j.jhydrol.2011.06.005.
Nesbitt, S.W., Anders, A.M., 2009. Very high resolution precipitation climatologies from the Tropical Rainfall Measuring Mission precipitation radar. Geophys. Res. Lett. 36, L15815. http://dx.doi.org/10.1029/2009GL038026.
Pal, I., Robertson, A.W., Lall, U., Cane, M.A., 2014. Modeling winter rainfall in northwest India using a hidden Markov model: understanding occurrence of different states and their dynamical connections. Clim. Dyn. 44 (3), 1003–1015. http://dx.doi.org/10.1007/s00382-014-2178-5.
Palazzi, E., von Hardenberg, J., Provenzale, A., 2013. Precipitation in the Hindu-Kush Karakoram Himalaya: observations and future scenarios. J. Geophys. Res. Atmos. 118 (1), 85–100. http://dx.doi.org/10.1029/2012JD018697.
Pang, H., Hou, S., Kaspari, S., Mayewski, P.A., 2014. Influence of regional precipitation patterns on stable isotopes in ice cores from the central Himalayas. Cryosphere 8 (2014), 289–301. http://dx.doi.org/10.5194/tc-8-289-2014.
Pellicciotti, F., Buergi, C., Immerzeel, W.W., Konz, M., Shrestha, A.B., 2012. Challenges and uncertainties in hydrological modeling of remote Hindu Kush–Karakoram–Himalayan (HKH) basins: suggestions for calibration strategies. Mt. Res. Dev. 32 (1), 39–50. http://dx.doi.org/10.1659/MRD-JOURNAL-D-11-00092.1.
Prakash, S., Mahesh, C., Gairola, R.M., 2013. Comparison of TRMM Multisatellite Precipitation Analysis (TMPA)-3B43 version 6 and 7 products with rain gauge data from ocean buoys. Remote Sens. Lett. 4 (7), 677–685. http://dx.doi.org/10.1080/2150704X.2013.783248.
Qazi, N.A., 1973. Water Resources Development in Suru Basin (Ladakh). 51. Vacant Press, Srinagar, India, p. 1973.
Qiu, J., 2008. China: the third pole, climate change is coming fast and furious to the Tibetan plateau. Nature 454, 393–396. http://dx.doi.org/10.1038/454393a 2008.
Rajeevan, M., Bhate, J., 2009. A high resolution daily gridded rainfall dataset (1971–2005) for meso-scale meteorological studies. Curr. Sci. 96, 558–562.
Rasmussen, R., Baker, B., Kochendorfer, J., Meyers, T., Landolt, S., Fischer, A.P., Black, J., Theriault, J.M., Kucera, P., Gochis, D., Smith, C., Nitu, R., Hall, M., Ikeda, K., Gutmann, E., 2012. How well are we measuring snow: the NOAA/FAA/NCAR winter precipitation test bed. Bull. Am. Meteorol. Soc. 93, 811–829. http://dx.doi.org/10.1175/BAMS-D-11-00052.1.
Reggiani, P., Rientjes, T.H.M., 2015. A reflection on the long-term water balance of the Upper Indus Basin. Hydrol. Res. 46, 446–462. http://dx.doi.org/10.2166/nh.2014.060.
Rivoirard, J., Wieland, K., 2001. Correcting for the effect of daylight in abundance estimation of juvenile haddock (*Melanogrammus aeglefinus*) in the North sea: application of kriging with external drift. ICES J. Mar. Sci. 58, 1272–1285.
Saha, K., 2010. Tropical Circulation Systems and Monsoons. Springer Heidelberg Dordrecht London New York http://dx.doi.org/10.1007/978-3-642-03373-5.
Sakai, A., Nuimura, T., Fujita, K., Takenaka, S., Nagai, H., Lamsal, D., 2014. Climate regime of Asian glaciers revealed by GAMDAM Glacier Inventory. Cryosphere Discuss. 8 (3629–3663), 2014. http://dx.doi.org/10.5194/tcd-8-3629-2014.
Schaake, J., 2004. Application of PRISM Climatologies for Hydrologic Modeling and Forecasting in the Western U.S. Proc. 18th Conf. on Hydrology, Seattle, WA, Amer. Meteor. Soc., 5.3. [Available online at http://ams.confex.com/ams/pdfpapers/72159.pdf.]
Schabenberger, O., Gotway, C.A., 2005. Statistical Methods for Spatial Data Analysis, Chapman an. CRC Press.
Schaefli, B., Hingray, B., Niggli, M., Musy, A., 2005. A conceptual glacio-hydrological model for high mountainous catchments. Hydrol. Earth Syst. Sci. 9 (1/2), 95–109. http://dx.doi.org/10.5194/hess-9-95-2005.
Scherler, D., Bookhagen, B., Strecker, M.R., 2011. Spatially variable response of Himalayan glaciers to climate change affected by debris cover. Nat. Geosci. 4, 156–159.
Schmidt, S., Nüsser, M., 2012. Changes of high altitude glaciers from 1969 to 2010 in the trans-Himalayan Kang Yatze Massif, Ladakh, Northwest India. Arct. Antarct. Alp. Res. 44 (1), 107–121. http://dx.doi.org/10.1657/1938-4246-44.1.107.

Schneider, U., Becker, A., Finger, P., Meyer-Christoffer, A., Zuise, M., Rudolf, B., 2013. GPCC's new land surface precipitation climatology based on quality-controlled in situ data and its role in quantifying the global water cycle. Theor. Appl. Climatol. 115, 15–40. http://dx.doi.org/10.1007/s00704-013-0860-x.

Shepard, D., 1968. A two-dimensional interpolation function for irregularly-spaced data. Proc. 23rd ACM National Conference. Association for Computing Machinery, pp. 517–524.

Shroder, J.F., Bishop, M.P., Copland, L., Sloan, V.F., 2000. Debris-covered glaciers and rock glaciers in the Nanga Parbat Himalaya, Pakistan. Geogr. Annal.: Ser. A Phys. Geogr. 82 (1), 17–31. http://dx.doi.org/10.1111/j.0435-3676.2000.00108.x.

SIHP, 1997. Snow and Ice Hydrology, Pakistan Phase-II Final Report to CIDA, Report No. 54, IDRC File No. 88-8009-00. International Development Research Centre, Ottawa, Ontario, Canada.

Singh, P., Kumar, N., 1997. Impact assessment of climate change on the hydrological response of a snow and glacier melt runoff dominated Himalayan river. J. Hydrol. 193 (1–4), 316–350.

Singh, P., Ramasastri, K.S., Kumar, N., 1995. Topographical influence on precipitation distribution in different ranges of Western Himalaya. Nord. Hydrol. 26, 259–284.

Syed, F.S., Giorgi, F., Pal, J.S., King, M.P., 2006. Effect of remote forcings on the winter precipitation of central southwest Asia part 1: observations. Theor. Appl. Climatol. 86 (1–4), 147–160. http://dx.doi.org/10.1007/s00704-0050217-1.

Tahir, A.A., Chevallier, P., Arnaud, Y., Ahmad, B., 2011. Snow cover dynamics and hydrological regime of the Hunza River basin, Karakoram Range, Northern Pakistan. Hydrol. Earth Syst. Sci. 15 (7), 2275–2290.

Tahir, A.A., Chevallier, P., Arnaud, Y., Ashraf, M., Bhatti, M.T., 2014. Snow cover trend and hydrological characteristics of the Astore River basin (Western Himalayas) and its comparison to the Hunza basin (Karakoram region). Sci. Total Environ. 505, 748–761. http://dx.doi.org/10.1016/j.scitotenv.2014.10.065.

Tobin, C., Nicotina, L., Parlange, M.B., Berne, A., Rinaldo, A., 2011. Improved interpolation of meteorological forcings for hydrologic applications in a Swiss Alpine region. J. Hydrol. 401, 77–89. http://dx.doi.org/10.1016/j.jhydrol.2011.02.010.

Treydte, K.S., Schleser, G.H., Helle, G., Frank, D.C., Winiger, M., Haug, G.H., Esper, J., 2006. The twentieth century was the wettest period in northern Pakistan over the past millennium. Nature 440 (7088), 1179–1182 (http://www.nature.com/nature/journal/v440/n7088/suppinfo/nature04743_S1.html).

UNESCO-SCOPE-UNEP, 2011. Third Pole Environment, Policy Briefs, No. 13 June 2011.

Verfaillie, E., van Lancker, V., van Meirvenne, M., 2006. Multivariate geostatistics for the predictive modelling of the surficial sand distribution in shelf seas. Cont. Shelf Res. 26, 2454–2468.

Wake, C.P., 1987. Spatial and Temporal Variation of Snow Accumulation in the Central Karakoram, Northern Pakistan, Paper 304. (MA), Wilfrid Laurier University, Ottawa, Canada. Retrieved from http://scholars.wlu.ca/etd/304.

Wake, C.P., 1989. Glaciochemical investigations as a tool for determining the spatial and seasonal variation of snow accumulation in the Central Karakoram, northern Pakistan,". Ann. Glaciol. 13, 279–284.

Wang, B., Lin, H., 2002. Rainy season of the Asian-Pacific summer monsoon. J. Clim. 15, 386–398.

Weedon, G.P., Balsamo, G., Bellouin, N., Gomes, S., Best, M.J., Viterbo, P., 2014. The WFDEI meteorological forcing data set: WATCH Forcing Data methodology applied to ERA-Interim reanalysis data. Water Resour. Res. 50, 7505–7514. http://dx.doi.org/10.1002/2014WR015638.

Wei, K., Gasse, F., 1999. Oxygen isotopes in lacustrine carbonates of West China revisited: implications for post glacial changes in summer monsoon circulation. Quat. Sci. Rev. 18, 1315–1334.

Weiers, S., 1995. Climatology for the NW Karakorum and Adjacent Areas. Statistical Analyses Involving Weather Satellite Images and Geographic Information System (GIS). Bonner Geographical Essays (in German) vol. 92. Bonn, p. 168.

Willmott, C.J., Rowe, C.M., Philpot, W.D., 1985. Small-scale climate maps: a sensitivity analysis of some common assumptions associated with grid-point interpolation and contouring. Amer. Cartogr. 12 (1), 5–16.

Wiltshire, A.J., 2014. Climate change implications for the glaciers of the Hindu Kush, Karakoram and Himalayan region. The Cryosphere 8, 941–958. http://dx.doi.org/10.5194/tc-8-941-2014 www.the-cryosphere.net/8/941/2014/.

Winiger, M., Gumpert, M., Yamout, H., 2005. Karakorum–Hindukush–Western Himalaya: assessing high-altitude water resources. Hydrol. Process. 19 (12), 2329–2338http://dx.doi.org/10.1002/hyp.5887.

Wu, G., Zhang, Y., 1998. Tibetan plateau forcing and the timing of the monsoon onset over south Asia and the south China sea. Mon. Weather Rev. AMS 126, 913–927. http://dx.doi.org/10.1175/1520-0493.

Yatagai, A., Kawamoto, H., 2008. Quantitative Estimation of Orographic Precipitation Over the Himalayas by Using TRMM/PR and a Dense Network of Rain Gauges. Vertical Heating Profiles From Satellites and Models. In: Krishnamurti, T.N., Goswami, B.N., Yatagai, A. (Eds.), SPIE Proceedings vol. 7148, 71480C. International Society for Optical Engineering. http://dx.doi.org/10.1117/12.811943.

Yatagai, A., Xie, P., 2006. Utilization of a rain gauge-based daily precipitation dataset over Asia for validation of precipitation derived from TRMM/PR and JRA-25. SPIE 2006, 6404–6453. http://dx.doi.org/10.1117/12.723829.

Yatagai, A., Kamiguchi, K., Arakawa, O., Hamada, A., Yasutomi, N., Kitoh, A., 2012. APHRODITE: constructing a long-term daily gridded precipitation dataset for Asia based on a dense network of rain gauges. Bull. Am. Meteorol. Soc. 93, 1401–1415.

Yihui, D., Zunya, W., 2008. A study of rainy seasons in China. Meteorog. Atmos. Phys. 100, 121–138. http://dx.doi.org/10.1007/s00703-008-02992 2008.

Yin, Z.-Y., Zhang, X., Liu, X., Colella, M., Chen, X., 2008. An assessment of the biases of satellite rainfall estimates over the Tibetan plateau and correction methods based on topographic analysis. J. Hydrometeorol. 9, 301–326.